HAZE REMOVAL ALGORITHM USING IMPROVED RESTORATION MODEL BASED ON DARK CHANNEL PRIOR

DAI ZHEN

FACULTY OF COMPUTER SCIENCE & INFORMATION TECHNOLOGY
UNIVERSITY OF MALAYA
KUALA LUMPUR

2019

HAZE REMOVAL ALGORITHM USING IMPROVED RESTORATION MODEL BASED ON DARK CHANNEL PRIOR

DAI ZHEN

DISSERTATION SUBMITTED IN PARTIAL FULFILMENT OF THE REQUIREMENTS FOR THE DEGREE OF MASTER OF COMPUTER SCIENCE

FACULTY OF COMPUTER SCIENCE AND INFORMATION TECHNOLOGY
UNIVERSITY OF MALAYA
KUALA LUMPUR

2019

UNIVERSITI MALAYA

ORIGINAL LITERARY WORK DECLARATION

Name of Candidate: DAI ZHEN

Registration/Matric No: WOA160029

Name of Degree: MASTER OF COMPUTER SCIENCE

Title of Project Paper/Research Report/Dissertation/Thesis ("this Work"): HAZE REMOVAL ALGORITHM USING IMPROVED RESTORATION MODEL BASED ON DARK CHANNEL PRIOR

Field of Study: Image Processing

I do solemnly and sincerely declare that:

(1) I am the sole author/writer of this Work;
(2) This Work is original;
(3) Any use of any work in which copyright exists was done by way of fair dealing and for permitted purposes and any excerpt or extract from, or reference to or reproduction of any copyright work has been disclosed expressly and sufficiently and the title of the Work and its authorship have been acknowledged in this Work;
(4) I do not have any actual knowledge nor do I ought reasonably to know that the making of this work constitutes an infringement of any copyright work;
(5) I hereby assign all and every rights in the copyright to this Work to the University of Malaya ("UM"), who henceforth shall be owner of the copyright in this Work and that any reproduction or use in any form or by any means whatsoever is prohibited without the written consent of UM having been first had and obtained;
(6) I am fully aware that if in the course of making this Work I have infringed any copyright whether intentionally or otherwise, I may be subject to legal action or any other action as may be determined by UM.

Candidate's Signature Date

Subscribed and solemnly declared before,

Supervisor's Signature Date

Name: Hamid Abdullah Jalab

Designation: Associate Professor

HAZE REMOVAL ALGORITHM USING IMPROVED RESTORATION MODEL BASED ON DARK CHANNEL PRIOR

ABSTRACT

In recent years, with the rapid development of social economy and the continuous improvement of people's living standard, the awareness of security precaution is becoming increasingly important. As an important tool for security work, video monitoring is widely used in traffic, outdoors, shopping malls and warehouses. However, in severe weather conditions, rain and haze have a large influence on the images obtained by video monitoring like the image contrast declines, color fades and edge blur. In this way, it is difficult to obtain the image contrast information, and it has a bad impact on the security work. So the clarity of images becomes very meaningful, and researchers start to pay attention to the field of image dehazing. Among many studies, the dark channel prior (DCP) dehazing algorithm is a major breakthrough in the field of image dehazing technology, and this algorithm has the advantages of simple, real-time and effective, while the limitation is that its shortcomings are mainly on the atmospheric scatting physical model over-reliance, and cannot be chosen to match the size of the filter temple, the lack of applicability of the sky and the image after the dark side. Based on the atmospheric physical model, this research proposed a haze removal algorithm using improved restoration model based on dark channel prior, which has good robustness to the bright sky regions, and also has a good effect on the edges. Firstly, the haze images were detected as having sky regions or having no sky

regions. Secondly, haze images that have sky regions were segmented into sky region and non-sky region. Then, the haze images that have sky regions and have no sky regions were dehazed respectively. Finally, the haze-free images were obtained. For the haze-free images obtained in this research, the subjective and objective evaluation criteria are adopted. Subjective evaluation is mainly in accordance with human visual standards, and the common objective evaluation criteria using "Image Quality Evaluator (NIQE)" and also compare the proposed result with other traditional methods.

Keywords: Image dehazing; dark channel prior; restoration model; Image Quality Assessment.

ABSTRAK

Dalam tahun-tahun kebelakangan ini, dengan perkembangan pesat ekonomi sosial dan penambahbaikan berterusan standard hidup rakyat, kesedaran mengenai langkah berjaga-jaga keselamatan menjadi semakin penting. Sebagai alat penting untuk kerja keselamatan, pemantauan video digunakan secara meluas dalam trafik, di luar, pusat perbelanjaan dan gudang. Walau bagaimanapun, dalam keadaan cuaca yang teruk, hujan dan jerebu mempunyai pengaruh besar pada imej-imej yang diperolehi oleh pemantauan video seperti penurunan kontras imej, pewarna warna dan kelebihan blur. Dengan cara ini, sukar untuk mendapatkan maklumat kontras imej, dan ia mempunyai kesan buruk terhadap kerja keselamatan. Oleh itu kejelasan imej menjadi sangat bermakna, dan para penyelidik mula memberi perhatian kepada bidang imej yang dehazing. Antara banyak kajian, algoritma dehazing kanal sebelumnya (DCP) merupakan terobosan besar dalam bidang teknologi hehaing imej, dan algoritma ini mempunyai kelebihan yang mudah, tepat masa dan berkesan, sementara batasannya adalah bahawa kekurangannya adalah terutamanya pada model atmosfera mengesan model fizikal yang berlebihan, dan tidak boleh dipilih untuk dipadankan dengan saiz kuil penapis, kekurangan kebolehgunaan langit dan imej selepas sisi gelap. Berdasarkan model fizikal atmosfera, penyelidikan ini mencadangkan algoritma penyingkiran jerebu menggunakan model pemulihan yang lebih baik berdasarkan saluran gelap sebelumnya, yang mempunyai keteguhan yang baik terhadap kawasan langit yang terang, dan juga mempunyai kesan yang baik pada tepi. Pertama, imej

jerebu dikesan sebagai kawasan langit atau tidak mempunyai kawasan langit. Kedua, imej jerebu yang mempunyai wilayah langit dibahagikan kepada rantau langit dan rantau bukan langit. Kemudian, imej jerebu yang mempunyai kawasan langit dan tidak mempunyai kawasan langit masing-masing. Akhirnya, imej bebas jerebu diperolehi. Untuk imej bebas jerebu yang diperolehi dalam kajian ini, kriteria penilaian subjektif dan objektif diterima pakai. Penilaian subjektif adalah selaras dengan piawai visual manusia, dan kriteria penilaian objektif bersama menggunakan "Penguji Kualiti Imej (NIQE)" dan juga membandingkan hasil yang dicadangkan dengan kaedah tradisional lain.

Kata kunci: Imej dehazing; saluran gelap sebelum; model pemulihan; Penilaian Kualiti Imej.

ACKNOWLEDGEMENTS

First and foremost, I would like to express a great thankfulness to my supervisor, Dr. Hamid A. Jalab, for his strong support, patient guidance and sincere encouragement over these two years of the courses and research. My supervisor gave me the opportunity to carry out my research with few obstacles. The comments from him had a significant influence on this study.

Then, I would like to thank the Faculty of Computer Science and Information Technology, University of Malaya for providing me with a great academic environment and also offering me a well-equipped laboratory.

Finally, I would like to express a special word of thanks to my wife and parents for their faithful, continuous support and motivating me throughout the research and offering me patient assistance during the writing of the thesis. Again, a special thanks to my roommates, Wang Ning and Liu Shirui who accompanied me for these two years.

TABLE OF CONTENTS

LIST OF FIGURES

LIST OF TABLES

LIST OF ABBREVIATIONS

CB	Color balance
DCP	Dark Channel Prior
e.g.	For Example
et al.	Et alibi
etc.	Etcetera
GHH	Global Histogram Homogenization
i.e.	That is
MATLAB	MATrix LABoratory
MRF	Makov Random Field
NIQE	Natural Image Quality Evaluator
Otsu	Maximum between-group variance method
PSF	Point Spread Function
RAM	Random Access Memory
RGB	Red, Green and Blue color space

CHAPTER 1

INTRODUCTION

1.1 Research Inspiration and Background

Nowadays, video monitoring is increasingly applied to various occasions, such as traffic violation to screening, valuables custody, special areas of monitoring, etc. Normally, video acquisition module can provide clearer video of monitoring, so as to realize monitoring of designated areas. But in the rainy, hazy and other bad weather conditions, it will be difficult for the camera to capture high quality videos. Thus, it can reduce the adaptability of the monitoring system and increase its security risks (Wang Y.C., 2011). Among all the bad weather, the frequency of haze is very high, and it can be seen that haze phenomenon has a great influence of human beings. At the same time, the haze has great interference with computer imaging. In the monitoring system and traffic network, whether video systems can work normally or not depends on the correctness and completeness of input image information (Dong C.P., 2017).

The loss of a lot of information in the original haze image will adversely affect many aspects of daily production and life. It is necessary to studying haze removal technology in order to highlight the image features that are more conducive to computer processing. The main goal is to restore the color and contrast that should normally be displayed in the original image, and try to restore a sharper image (Mao T.Y., 2017).

The effect of haze on light is relatively large, mainly reflected in the absorption, scattering and radiation effects of light. The effect of haze on the wavelength and

scattering of visible light is relatively large, which will reduce the sharpness of the image. The scattering of light divided into two models. One is single scattering model, and the other one is multiple scattering model. In the case of haze, the spacing of small particles suspending in the air is much larger than the small particles themselves, so in this case the scattering of the spacing of small particles can be ignored, and this can be viewed as a scattering model. For the image formation, the brightness of light increases with distance, and the closer the distance is, the smaller the brightness will be. On the contrary, the further away the distance is, the greater the attenuation of light. That is why in the haze weather, people can see the near-distance scenery, but cannot see the distant scenery.

There are two important methods for haze removal in image processing contemporarity. One is haze image enhancement based on image processing, and the other one is haze image restoration based on physical models.

The method of haze image enhancement based on image processing mainly improves the visual effect of images by improving the contrast of haze images and highlight image details, so as to achieve the goal of image dehazing. It is important to note that this method does not take into account the images' quality, and using this method to dehaze may cause a certain loss of the image highlights information, but this method is widely used. The researchers combined traditional techniques with a deeper level of enhancing image contrast technology to form a more common technique used image enhancement method, including histogram homogenization, wavelet analysis, Retinex algorithm, etc.

The method of haze image restoration needs to study the physical process of the degradation of haze image quality that based on the physical models in firstly. The physical degradation model is established through research, and then the parameters in the model are estimated to reduce the distortion in the process of degradation, and finally the high quality image without haze after recovery is obtained. At the key point of this method, the degradation model is established and parameters in the model are estimated accurately. The image restoration technology based on physical model is mainly divided into multiple image restoration technology and single image restoration technology. Multiple image restoration technology is based on multiple images extracted from different weather conditions in the same scene, but time limit requirement is relatively strict. Oakley and Satherley (1988) proposed the theory of modified daylighting map for image restoration at the earliest. Then on the basis, Narasimhan and Nayar (2003) purposed the theory of multiple image restoration. However, the calculation of this method is very large, and it will have an obvious effect on the same scene. So the researchers proposed a single image restoration technology designed (Wang Y.C., 2011). There are many researches in haze removal based on single image restoration. For example, Tan R. (2008) used MRF model to construct the cost function of edge strength and used graph cut method to estimate the best illumination. Fattal R. (2008) proposed a method that used independent component analysis to estimate scene irradiance.

There are many researches in haze removal of single image model based on prior information (Mao T.Y., 2017). At present, most of the studies focus on the dehazing

method based on dark channel prior that He Kaiming proposed in 2009. In the non-sky region of haze-free images in outdoor, some pixel values are very low on a color channel in three R.G.B channels. The transmittance is roughly estimated using the local minimum filtering algorithm, then image soft matting is used to refine the transmittance and got the corresponding transmission rate distribution map. For bright sky regions where the dark channel prior rule fails, some solutions are to operate as a whole, without differentiating between sky and non-sky regions. The focus of this research is to distinguish between sky and non-sky regions in haze images and use an improved restoration model based on dark channel prior for haze removal in single images, so as to realize the image dehazing function quickly and effectively.

1.2 Problem Statement

Dehazing processing is one of the hot research fields in image processing (Liu, 2016). Based on the current literature information on dehazing processing, image restoration technology is one of the most widely used algorithms. It uses some model algorithms to obtain a clear image without haze. This technology is highly targeted, so the image effect after dehazing is very significant, and the estimation of parameters in the model is the key to this method (Lin, 2017). Among many image restoration technologies, the algorithm of image dehazing based on dark channel prior (He, 2011) is the most representative one. This algorithm has been recognized by many researchers, and it has obtained a good effect on dehazing. On the basis of dark channel

prior theory, researchers have proposed many new algorithms. According to the literatures in recent years, high-order Makov Random Fiends (Leng & Li, 2017), improved media filtering algorithm instead of soft matting (Fan, 2016), and energy function (Shi, et al, 2017) are used, which are all based on dark channel prior. But they all have some disadvantages, such as blurred edge image details during processing, and poor dehaizng effect on bright regions. Therefore, this research proposed a dehazing method based on dark channel prior, which aims to solve the following image dehazing limitations:

i. The blurred edge image details during processing (Figure 1).

(a) (b)

Figure 1.1: The blurred edge limitation: (a) Input image, (b) Output image of DCP

ii. The distortion effect in sky region and large bright region (Figure 2).

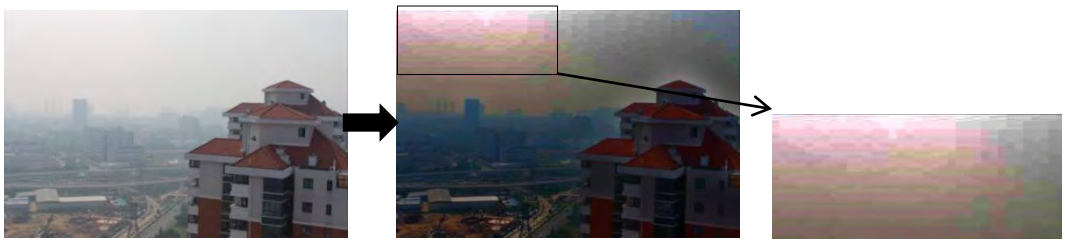

(a) (b)

Figure 1.2: The sky region limitation: (a) Input image, (b) Output image of DCP

1.3 Research Questions

Several research questions have been formulated to fill in as a rule to direct this research and to accomplish the research goals at different phases:

i. How does image restoration technology work in image dehazing?

ii. How to create a robust algorithm to remove the haze of image also has a good effect on the edges?

iii. How to evaluate the result obtained by this proposed algorithm?

1.4 Aim and Objectives of the Research

Every research has its own goal and achievement. This research aims to develop a haze removal algorithm using improved restoration model based on dark channel prior. And this research is conducted based on the following objectives:

i. To analyse the dehazing algorithm based on image restoration.

ii. To propose an improved image dehazing algorithm based on dark channel prior,

which has a good effect on sky, brightness regions and edges.

iii. To evaluate the proposed algorithm by using both the subjective and objective evaluation, where NIQE is used in objective evaluation, and subjective evaluation is mainly based on human judgment of the sharpness of the image after dehazing.

1.5 Scope of Work

In order to conduct this research in a well-structured manner, the experimental work is divided into several stages:

i. **Research study:** The limitations and drawbacks of haze removal technologies based on dark channel prior are identified from the result of the literature review. Data is collected from many related publications including journals and conference papers. After studying, a conclusion is reached that which areas require changes as far as the distortion in sky and brightness region and the blur edges during processing.

ii. **Methodology:** In this stage, the research comprises of the plan and implementation of haze removal method using improved restoration model based on dark channel prior.

iii. **Dataset:** The digital image database for this research was selected from two parts. One is from the Internet that the haze images are widely used in the field of haze removal. The other one is from the haze images that are captured by monitoring systems.

iv. **Conduction experiments:** In terms of robustness and treatment efficiency, the performance of the proposed method is evaluated and compared with other traditional methods. Quantitative and qualitative results are achieved based on the dataset.

1.6 Research Contributions

The images collected in the haze are due to the scattering of atmospheric particles, and can result in the image color saturation and contrast reduction As a result, the objects are difficult to recognize. This not only affects the visual effect, but also reduces the visual ability of the image. What's worse, it affects the later processing of the image. Therefore, it is necessary to use the image dehazing technology to process haze images to obtain the images with high resolution and contrast. The image dehazing technology based on image restoration has been paid close attention to by many scholars.

With the development of single image dehazing algorithm, especially since dark channel prior knowledge has been put forward, single image technology has become more and more mature, processing efficiency has become higher and higher, and the quality of dehazing image has become better and better. However, when focusing on the algorithm, several problems were also found, such as the loss of details in the dehazing images, the poor effects of dehazing on the bright areas, poor edge protection, color distortion, etc.

This research makes some changes under the support of these theoretical knowledge, and aims to propose an improved algorithm for haze removal using improved restoration model based on dark channel prior. The proposed algorithm will effectively solve the problem of failure that contains large areas of sky or white objects in haze images that use dark channel prior dehazing algorithm, thereby enlarging the application scope of the dark channel. In addition, the proposed algorithm will have good edge retention characteristics. The resulting image will have higher resolution and visibility and also have better values in "NIQE" than other traditional haze removal methods.

1.7 Thesis Outline

There are five chapters in this research. All chapters are structured according to the proposed algorithm. Each chapter is structured as follows:

Firstly, Chapter 2 mainly introduces some classical haze removal algorithms and the haze removal algorithm based on dark channel prior. In this chapter, the relevant classification and atmospheric scattering model in the field of haze removal algorithm are briefly introduced. Similarly, the haze removal algorithm using sky segmentation based on dark channel prior is also described in this chapter.

Secondly, in Chapter 3, the details of the proposed approach are covered. The proposed approach consists of sky region detection and segmentation, two different haze removal algorithms for the haze images that have sky region and have no sky

region, and color balance.

Then, Chapter 4 begins with the result arrangement of the proposed haze removal method. Moreover, Chapter 4 decorates the result of the proposed method against the analyzed problems and assesses them compared with other traditional haze removal methods.

Finally, in Chapter 5, the outline of the proposed haze removal method is given. In addition, a concise summary of the contents is given and some suggestions are proposed.

CHAPTER 2

LITERATURE REVIEW

2.1 Background

In the previous chapter, the importance and motivation of haze removal has been presented. This chapter proceeds with brief explanation of haze removal based on image enhancement and image restoration, atmospheric physical model, haze removal method in image restoration based on dark channel prior, and a current research in sky segmentation haze removal techniques.

This chapter is organized as follows. Section 2.2 explains the techniques in image enhancement. Section 2.3 explains the techniques in image restoration and describes image restoration technology in multiple image and single image. Section 2.4 explains the atmospheric physical model. Section 2.5 introduces and analyzes the haze removal technology based on dark channel prior. Section 2.6 describes a haze removal method based on sky segmentation.

2.2 Haze Removal Method Based on Image Enhancement

At present, there are two effective methods in the field of haze removal. One is based on image enhancement, and the other one is image restoration based on physical model. The image enhancement method is mainly used to achieve the purpose of haze removal by improving the image contrast and details. But this approach blindly changes the information of the haze image, and it also destroys the original information

of the haze image when it has the effect of removing the haze. Among the algorithm which utilize image enhancement for haze removal, the ones which are widely applied and representative are the histogram homogenization algorithm (Shang H L, et al, 2015), the homomorphic filtering algorithm (Seow M J, & Asari U K, 2006), the Retinex algorithm (Tang L, et al, 2011) and the wavelet transform algorithm (Russo F, 2002), etc.

2.3 Haze Removal Method Based on Image Restoration

The image restoration method based on physical model firstly analyzes the process of image degradation according to the cause of image quality degradation in haze weather. Secondly this process is restored through physical modeling. Then the parameters needed in the physical model are obtained in the haze image and the missing parameter values are estimated. Finally, the haze-free image is restored (Xu Z. X., 2014). The kind of method is more targeted, and the obtained haze removal effect is more natural and the information loss is less. However, the most important step in this kind of method is the estimation of each parameter in the model.

The method based on image restoration is a popular haze removal algorithm. From the image classification, it is mainly classified into multiple image restoration technology and single restoration technology.

Multiple image restoration technology is based on multiple images extracted from different weather conditions in the same scene, but time limit requirement is relatively

strict. The theory of modified daylighting map was proposed by Oakley & Satherley (1988) for image restoration at the earliest. Then on that basis, Narasimhan et al. (2003) purposed the theory of multiple image restoration. However, the calculation of this method is very large, and it will have an obvious effect in the same scene.

So the researchers propose a single image restoration technology designed to reduce computation time and to avoid environmental restrictions on image restoration. Based on the prior information, haze image restoration method is mainly aimed at the single image with haze, according to the change of the concentration of haze, to achieve the purpose of complete haze removal. Tan R. (2008) proposed an algorithm for haze removal using prior information. That is, the haze-free image is higher in contrast to the haze image, and at the same time, the influence of ambient light tends to be smoothed as the depth of the scene decreases. Therefore, under the condition of incomplete restoration of the original reflectivity of the scene, the local information contrast can be maximized by using prior information, and the clear haze-free image can be finally obtained. The success of this method is that the gray haze image and the color haze image can be processed.

Fattal R. (2008) used "the propagation of light is not related to the part of the surface of the target surface" as prior information, and estimated the radiation level of the scene at the beginning, and then the propagation image was derived. It is a haze removal algorithm based on image restoration and statistical law of mathematics, and it uses a traditional method in image dehazing. In this method, source singles are separated from multiple singles. The signal has N variables (y_1, y_2 ,..., y_n). The

observed variables ($x = (x_1, x_2, \dots, x_n)^T$) are obtained after linear combination,

$$x_i = a_{i1}y_1 + a_{i2}y_2 + \cdots + a_{in}y_n (i = 1,2, \dots, n) \tag{2.1}$$

Let's set $y = (y_1, y_2, \dots, y_n)^T$, $A = [a_{ij}]$, it is equal to $x = Ay$. And sets hybrid matrix W, $y = Wx$, $x = As$. Since *s* and *A* are unknown, the value of *W* is evaluated by the independent component analysis method.

Fattal's algorithm is based on the fact that the propagation of light and the reflectivity of the target surface are independent of each other,

$$I = ltR + A(1 - t) \tag{2.2}$$

where, *R* is the reflection factor of target object surface, *l* is the reflected light.

$$\eta = \frac{(I,A)}{||R'|| \cdot ||A||} \tag{2.3}$$

$$l' = ||R'||l \tag{2.4}$$

$$I_A = tl'\eta + (1 - t)||A|| \tag{2.5}$$

where, I_A is the projection in the direction of *A* and R'.

The transmittance t can be derived from formula 2.4 and 2.5,

$$t = 1 - \frac{(I_A - \eta I_{R'})}{||A||} \tag{2.6}$$

The haze-free image is obtained according to η and the transmittance *t*.

2.4 Atmospheric Physical Model

The scattering phenomenon occurs when light travels through the medium, and the accurate physical model to describe the scattering phenomenon is very complicated and difficult to obtain. McCartney proposed the widely used atmospheric scattering

model, whose basic idea is that the atmospheric model in haze weather mainly consists of two parts, namely attenuation model and ambient light model (McCartney E. J., 1975).

In the case of haze weather, the radiation energy transferred from the scene to the imaging equipment is generated by the combined action of the rest part and the ambient light part after the radiation energy of the scene scattered and attenuated by the particles in the atmosphere. This phenomenon is shown in Figure 2.1. As can be seen from the figure, the light captured by the imaging equipment during haze is mainly divided into two parts. One is the remainder of the reflected light by the atmosphere (solid line section), and the other one is the remainder of the scattering attenuation of the ambient light by the atmosphere (dotted line).

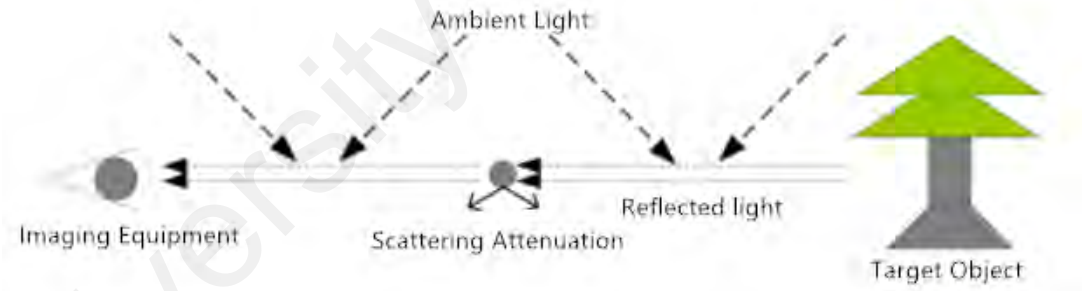

Figure 2.1: Imaging model of haze image

By analyzing the haze weather imaging model and carrying out the mathematical modeling, the accurate mathematical description of the haze weather imaging model can be obtained.

The attenuation model is used to describe the process of the reflected light of scene objects entering the imaging equipment directly through atmospheric medium, which indicates that the reflected light intensity of scene objects entering the imaging

equipment will decrease with the increase of propagation distance (Narasimhan S G & Nayar S K, 2002). If the incident light is assumed to be parallel, then the intensity of reflected light can be obtained according to the attenuation as follows:

$$E(d,\lambda) = E_0(\lambda)e^{-\beta(\lambda)d} \tag{2.7}$$

where, λ is the wavelength of light, β is atmospheric scattering coefficient or attenuation coefficient. *d* is the distance between the scene and imaging equipment. E_0 is the reflected light intensity at a distance *(d)* of 0. *E* is the reflected light intensity that enters the imaging equipment. As the distance increases, the scattering effect of small water droplets and suspended particulate matter on reflected light will increase greatly, and this makes the intensity of light entering the imaging equipment decrease significantly.

It can be seen from the haze weather imaging model that the light enters the imaging equipment includes not only the reflected light of the scene but also the ambient light. The ambient light model is used to describe the process of the ambient light entering the imaging equipment in the imaging environment (Narasimhan S G & Nayar S K, 2002). The formula of ambient light intensity obtained according to the ambient light mode is as follows:

$$L(d,\lambda) = L_\infty(\lambda)(1 - e^{-\beta(\lambda)d}) \tag{2.8}$$

where, λ is the wavelength of light, β is atmospheric scattering coefficient or attenuation coefficient. *d* is the distance between the scene and imaging equipment. *L* is the ambient light intensity that entered the imaging equipment. L_∞ is the ambient light intensity that is infinitely distant from the imaging equipment. As the distance *(d)*

increases, $e^{-\beta(\lambda)d}$ decreases, and $L(d,\lambda)$ increases. That is, as the distance increases, the intensity of ambient light entering the imaging equipment increases.

When light propagates in the medium, it will attenuate under the influence of particles suspending in the medium. Different wavelengths of light are affected to different degrees by particles in the medium, and this degree is determined by the attenuation coefficient (β). The attenuation coefficient is related to the transverse geometrical linearity of the scattered particles in the medium and the wavelength of incident light. Mie Scattering Law describes this relationship (Narasimhan S G. & Nayar S K., 2002).

Table 2.1 shows the relationship between particle type, radius and spatial concentration under different weather conditions.

Table 2.1: The Scattering Particle Size and Spatial Distribution Concentration in Different Weather Conditions

Weather Situation	**Particle Type**	**Particle Radius(μm)**	**Spatial Concentration(cm^{-3})**
Sunny Day	Molecule	10^{-4}	10^{19}
Mist	Suspended Particle	10^{-2}~1	10^{3}~10
Haze Weather	Water Droplet	1~10	100~10
Cloud	Water Droplet	1~10	300~10
Rain	Water Drop	10^{2}~10^{4}	10^{-2}~10^{-5}

The scattering under haze conditions is the large particle scattering, which is the

ultimate state of Mie Scattering. In this case, the attenuation coefficient (β) is independent of the wavelength (λ).

To sum up, a simplified atmospheric scattering model of haze image can be obtained as follows.

$$I(d) = E(d) + L(d) = E_0 e^{-\beta d} + L_\infty (1 - e^{-\beta d}) \quad (2.9)$$

where, β is the atmospheric scattering coefficient. d is the distance between imaging equipment and scene. E_0 is the intensity of reflected light without atmospheric attenuation. L_∞ is the ambient light intensity at an infinite distance from the imaging equipment.

Currently, in the field of computer vision, the formula of Koschmieder is commonly used to describe haze weather imaging model (Narasimhan S G & Nayar S K, 2000),

$$I(x) = J(x)t(x) + A(1 - t(x)) \quad (2.10)$$

where, *I(x)* is the haze image. *J(x)* is the haze-free image. *A* is the atmospheric light. *t(x)* is the transmittance of medium ($t(x) = e^{-\beta d(x)}$). *J(x)t(x)* is the damping item. *A(1-t(x))* is the atmospheric scattering light. β is the atmospheric scattering coefficient. *d(x)* is the depth of scene. Combined with the atmospheric scattering model, some mainstream haze removal algorithms, such as the algorithm based on dark channel prior (He K M., et al, 2009), restore the haze-free image by reverse solving.

2.5 Haze Removal Technology Based on Dark Channel Prior

The algorithm based on dark channel prior principle takes dark channel as prior information, and the haze-free image is obtained based on the physical model (He K M,

et al. 2011).

2.5.1 Dark Channel Prior Principle

He Kaiming (2011) proposed prior information based on the statistical law of a large number of outdoor haze-free images. That means for most haze-free images of outdoor non-sky regions, there are at least pixels with a very low color channel value. The dark channel prior principle is shown in formula 2.11,

$$J^{dark}(x) = \min_{y \in \Omega(x)} \left(\min_{c \in \{r,g,b\}} J^c(y) \right) \quad (2.11)$$

Where, J^c is each channel of the color images. $\Omega(x)$ is a window centered on pixels x. J^{dark} goes to 0 by using the dark primaries principle. Figure 2.2 shows sample of dark channel images.

(a)

(b)

Figure 2.2: Sample of dark channel image: (a) Haze images, (b) Dark channel images

2.5.2 Transmittance Estimation

The transmittance is estimated according to the dark channel prior principle and the haze image physical model. The atmospheric light value A is assumed to be known, and the transmittance within a local area is a constant value,

$$\frac{I^c(x)}{A^c} = t(x)\frac{J^c(x)}{A^c} + 1 - t(x) \tag{2.12}$$

The following formula can be obtained by performing the minimization operation,

$$\min_{y\in\Omega(x)}\left(\min_c \frac{I^c(y)}{A^c}\right) = \tilde{t}(x)\min_{y\in\Omega(x)}\left(\min_c \frac{J^c(y)}{A^c}\right) + 1 - \tilde{t}(x) \tag{2.13}$$

$$\tilde{t} = \frac{1-\min_c \frac{I^c(y)}{A^c}}{1-\min_c \frac{J^c(y)}{A^c}} \tag{2.14}$$

The following formula can be obtained according to the dark channel prior,

$$J^{dark}(x) = \min_{y\in\Omega(x)} \left(\min_{c\in\{r,g,b\}} J^c(y) \right) = 0 \tag{2.15}$$

So the formula 2.14 can be transformed into,

$$\tilde{t}(x) = 1 - \omega \min_{y\in\Omega(x)} \left(\min_c \frac{I^c(y)}{A^c} \right) \tag{2.16}$$

where, $\omega \in [0,1]$, the parameter ω is introduced to retain a certain depth of field to make the image more natural and realistic.

In order to improve the efficiency of haze removal based on dark channel prior, Dr. He Kaiming used guided filtering instead of soft matting (He K M., et al, 2011). And he used the haze image as the guided map to filter the transmittance and retain the details, so as to optimize the transmittance.

The model of guided filtering is shown as follows:

$$q_i = \sum_j w_{ij}(I) p_j \tag{2.17}$$

where, p is the input image. q is the output image. i and j are the coordinates of pixels. I is the guided map of guided filtering. ω_{ij} is kernel filter.

Guided filtering is based on the assumption that its filtered is a linear transformation of the guided map,

$$q_k = a_k I_i + b_k, \forall i \in \omega_k \tag{2.18}$$

where, k is the pixel center. ω_k is the local window.

a_k and b_k are a pair of linear coefficients, because it needs the least difference between the input image and the output image, so

$$E(a_k, b_k) = \sum_{i \in \omega_k}((a_k I_i + b_k - p_i)^2 + \varepsilon a_k^2) \tag{2.19}$$

where, ε is the regularization parameter

$$\begin{cases} a_k = \frac{\frac{1}{|\omega|}\sum_{i \in w_k} I_i p_i - \mu_k \bar{p}_k}{\sigma_k^2 + \varepsilon} \\ b_k = \bar{p}_k - a_k \mu_k \end{cases} \tag{2.20}$$

After all the results are solved, the final filtering results can be obtained,

$$\begin{cases} q_i = \frac{1}{|\omega|}\sum_{i \in \omega_k} I_i p_i - \mu_k \bar{p}_k \\ q_i = \bar{a}_i I_i + \bar{b}_k \\ \bar{a}_i = \frac{1}{|\omega|}\sum_{i \in \omega_k} a_k \\ \bar{b}_k = \frac{1}{|\omega|}\sum_{i \in \omega_k} b_k \end{cases} \tag{2.21}$$

The kernel coefficients of the guided filtering are shown below:

$$W_{ij}(J^g) = \frac{1}{|\omega|^2}\sum_{k:(i,J) \in \omega_k}(1 + \frac{(J_i^g - \mu_k)(J_j^g - \mu_k)}{\sigma_k^2 + \varepsilon}) \tag{2.22}$$

where, J_g is the guided map. σ^2 is the variance. μ_k is the mean value. $|\omega|$ is the number of pixels in ω_k.

2.5.3 Calculate the Value of Atmospheric Light

Firstly, the first 0.1% pixels in the dark channel map been selected according to the brightness value. And then the value of the maximum brightness points is found in the coordinates of original haze image corresponding to these positions in dark channel image.

2.5.4 Restore the Haze-free Image

Finally, formula 2.23 is used to get the image after haze removal,

$$J(x) = \frac{I(x) - A}{max(\bar{t}(x), t_0)} + A \tag{2.23}$$

Figure 2.3 shows samples of haze free images after applying DCP algorithm.

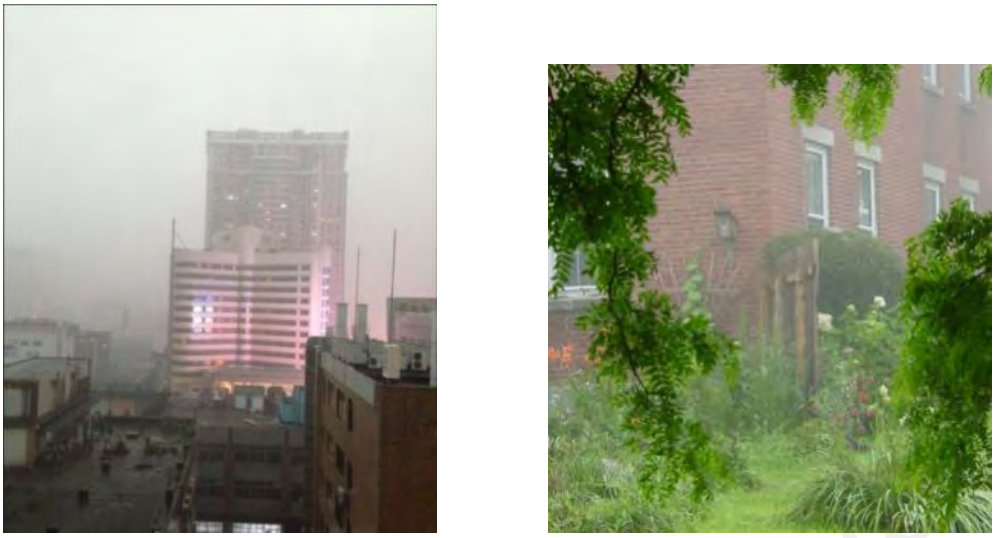

(a)

(b)

Figure 2.3: Samples of haze free image after applying DCP: (a) Haze images, (b) Haze free images

2.6 Single Image Haze Removal Using Segmentation of Otsu

In order to solve the issue of low estimated transmittance in the sky regions by dark channel prior, an algorithm for haze removal based on an improved recursive segmentation derived from Otsu algorithm was proposed (Wu Y H., et al, 2017). Under the thought of image segmentation, the method is accurate to separate sky region via the improved recursive segmentation of Otsu rule, which is combined with the normalized gray values of the dark channel map to amend the estimation for the transmission in the sky region.

Assuming that the haze image contains L gray values, the probability of gray value appearing in the haze image is

$$P_i = \frac{n_i}{N}, i = 0,1, \dots, L-1 \tag{2.24}$$

where, n_i is number of pixels of gray values i, and N is total number of pixels in haze image. Haze image is divided into sky region and non-sky region by the threshold value x. Sky region $S = \{1, 2, \dots, x\}$, non-sky region $B = \{x+1, x+2, \dots, L\}$.

Firstly, let's set x is segmentation threshold value, ω_S and ω_B are the gray probabilities of sky region and non-sky region.

$$\omega_S = \sum_{i=0}^{x} P_i \quad \omega_B = \sum_{i=x+1}^{L-1} P_i \tag{2.25}$$

ω_S and ω_B are used to solve the average gray value μ_S of the sky region and the average gray value μ_B of the non-sky region.

$$\mu_S = \frac{\sum_{i=0}^{x} i \cdot P_i}{\omega_S} \quad \mu_B = \frac{\sum_{i=x+1}^{L-1} i \cdot P_i}{\omega_B} \tag{2.26}$$

Suppose a distance measurement $d^2(x)$, the distance between sky region and non-sky region increases with the increase of distance measurement, and the

segmentation accuracy increases accordingly (Guo X, 2015). However, while improving the distance measurement, the distance between each pixel and the center of the class should be reduced to achieve good pixel cohesion. The quality of cohesion is measured by the average variance of sky region and non-sky region.

$$d^2(x) = (\mu_S - \mu_B)^2 \tag{2.27}$$

$$\delta_S^2 = \frac{1}{\omega_S}\sum_{i=0}^{X}(i-\mu_S)^2\omega(i) \tag{2.28}$$

$$\delta_B^2 = \frac{1}{\omega_B}\sum_{i=X+1}^{L-1}(i-\mu_B)^2\omega(i) \tag{2.29}$$

where, δ_S^2 is the average variance of sky region, and δ_B^2 is the average variance of non-sky region.

The threshold value obtained by class distance and cohesion is obtained as below:

$$G(x) = \frac{\omega_S\omega_B d^2(x)}{\delta_S^2(x)+\delta_B^2(x)} = \frac{\omega_S\omega_B(\mu_S-\mu_B)^2}{\delta_S^2(x)+\delta_B^2(x)} \tag{2.30}$$

When *G(x)* is the maximum value, and *x* is the optimal threshold value *X*

$$X = arg\ \max_{0\le i\le L-1} \frac{\omega_S\omega_B(\mu_S-\mu_B)^2}{\delta_S^2(x)+\delta_B^2(x)} \tag{2.31}$$

After obtaining the threshold of sky segmentation, the specific algorithm for haze removal is shown in the Figure 2.4.

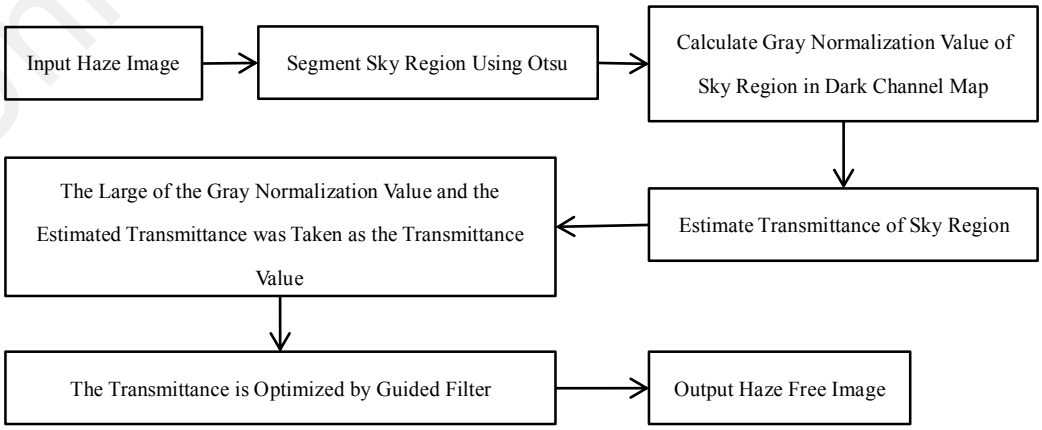

Figure 2.4: Steps of method of single image haze removal using an improved recursive segmentation of otsu

The recovered image preserves the true color and exhibits natural restoration between the boundary region. In order to effectively deal with the color distortion and halos appearing in the sky region, this algorithm broadens the application of dark channel prior to a certain extent, which has a great prospect for processing outdoor haze images. However, in some specific haze images, the problem of image distortion still exists when this algorithm is used to process (Wu Y H, Pan C, et al. 2017).

2.7 Summary

This chapter mainly introduces two mainstream haze removal theories, and analyzes the haze removal theory based on image restoration in details by introducing the haze removal algorithm based on dark channel prior, and finally introduces a haze removal algorithm based on sky region segmentation in recent five years. Based on the literature in this chapter, a new haze removal algorithm that based on the atmospheric scattering model and sky region segmentation is proposed in the next chapter.

CHAPTER 3

RESEARCH METHODOLOGY

3.1 Introduction

This chapter presents the complete methodology of the proposed haze removal algorithm using improved restoration model based on dark channel prior scheme. The chapter is divided into two sections for better explanation of the proposed method. Firstly, the analysis of research requirement is explained. Secondly, brief description of the research design and implementation is described. The proposed method in this study is a haze removal algorithm using improved restoration model based on dark channel prior. The proposed method divides the sky region of haze image, and optimizes the transmittance and the atmospheric light value. The results show that the proposed method is robust to large bright and sky regions. This chapter proceeds as the following sections. In section 3.2, 3.3, 3.4 and 3.5, brief discussion of research requirement analysis, general structure of the proposed algorithm, the specific and complete research design and implementation, and summary of the whole chapter are described respectively.

3.2 Research Requirement Analysis

At the beginning of the experiment, requirement analysis should be completed first. It should be done before developing the proposed algorithm. Sufficient analysis of the research requirements will make the subsequent algorithm research more smooth.

Figure 3.1 provides better illustration of this section.

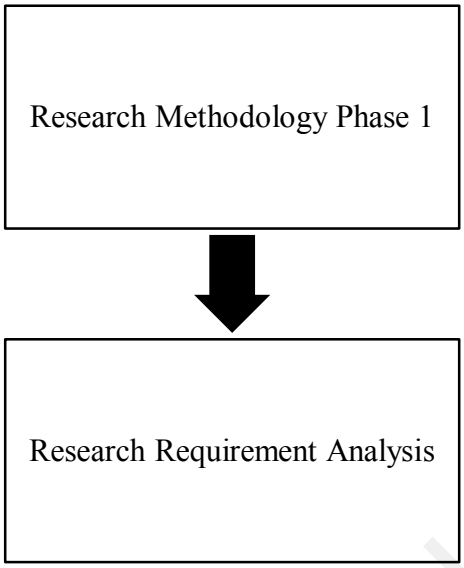

Figure 3.1: The first phase of research methodology

Review of existing methods and selecting a suitable scope to develop the proposed method are two activities in requirement stage. They are briefed as follows:

i. Existing methods review and compare

This step is the foundation of the proposed method in the research work. Related research literature is reviewed, and in-depth analysis is done to explore issues of the existing haze removal method based on dark channel prior. From chapter 2, brief review on existing literature helps to identify problem statement and it also helps to set research objectives. Moreover, analysis of drawbacks, limitations and advantages of existing literature helps to set the research aim.

ii. Selecting scope to develop proposed haze removal method based on dark channel prior

A comprehensive literature review is done to select scope of this research and the structure of the proposed haze removal algorithm. And an appropriate programming language is essential to implement and simulate any algorithm. Therefore, MATLAB is

used in this research as an experimental and programming tool. MATLAB is a high-level language, and it is mostly used in engineering calculation, control design, single processing and communication, image processing, single detection, etc. Based on the problem statement, the identified scope of the proposed algorithm can be given as follows:

- The proposed method can process haze image, and also can support RGB image.
- Can able to work with varied image.
- This method can remove the haze in the haze image well.
- The proposed method has a good effect in the sky region and also has a good effect in the edges.

3.2.1 Dataset

The haze weather is so pervasive and it is especially severe in some developing countries. So there is no particular dataset for these haze images. The haze images used in this research are different from some datasets in other image processing fields. It is just a image or video taken from the haze weather. It is not artificially modified, nor does it contain complex image information. Since this research only focuses on the haze removal of a single image, the dataset of this research mainly comes from two ways:

- The dataset was frequently used in previously researches based on DCP

The haze images previously used in the field of image haze removal are also used in this research. These haze images have typical characteristics of this research field,

some of them have rich scene information, and some are captured under different scenes. Figure 3.2 shows some haze images that have been widely used in previous studies, some of which will be used in this study.

(a)

(b)

(b)

(c)

Figure 3.2: The samples of haze image: (a) With sky region, (b) Without sky region, (c) Scenic spots

- The dataset captured in different scenes in real life

Haze removal technology is widely used in many fields of our life, and one important area is dehazing of images captured by monitoring. The images of Figure 3.3 were taken under monitoring in haze weather, and they will be used in this study.

Dehazing of these images taken by monitoring will be helpful for later image processing.

(a)

(b)

Figure 3.3: Samples of haze image: (a) Building, (b) Highway

3.3 General Structure of the Proposed Algorithm

This section presents the main structural design of the proposed haze removal method based on dark channel prior and explains the full implementation phase. As an outcome of constructing the method, the designed structure will be transformed into machine language. The following section will explain the full steps of the proposed algorithm.

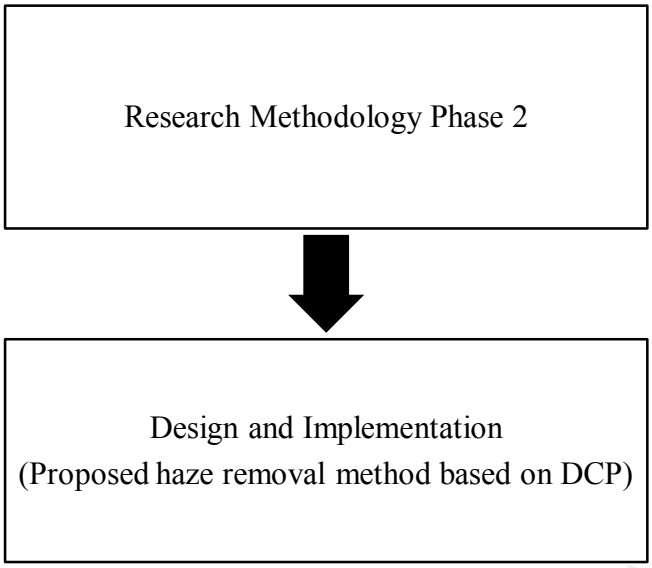

Figure 3.4: The second phase of research methodology

This section will provide justification for using the proposed method as shown in Figure 3.4. The proposed method is designed to remove the haze in haze images. In order to remove the haze, many techniques such as image segmentation, image filter and color balance are needed.

This section will present the procedural description of the proposed haze removal method based on dark channel prior. The proposed method in this research is a haze removal algorithm using an improved restoration model based on dark channel prior. Firstly, the input haze image is identified and segmented into the sky region that uses gradient and brightness information of image. Secondly, the haze image with sky region is processed with the method of dehaze-1, and the haze image without sky region is processed with the method of dehaze-2. The detailed steps and the output of each step of dehaze-1 and dehaze-2 will be described in this section. Then, the haze image is processed with color balance. Finally, output the haze-free image.

The whole proposed haze removal method can be described as follows (Figure 3.5):

i. Input the haze image.

ii. Sky region detection and segmentation (using the method of dehaze-1 to the original haze image which has sky region, using method of dehaze-2 to the original haze image which has no sky region).

iii. Dehaze.

iv. Image color balance.

v. Output the haze-free image.

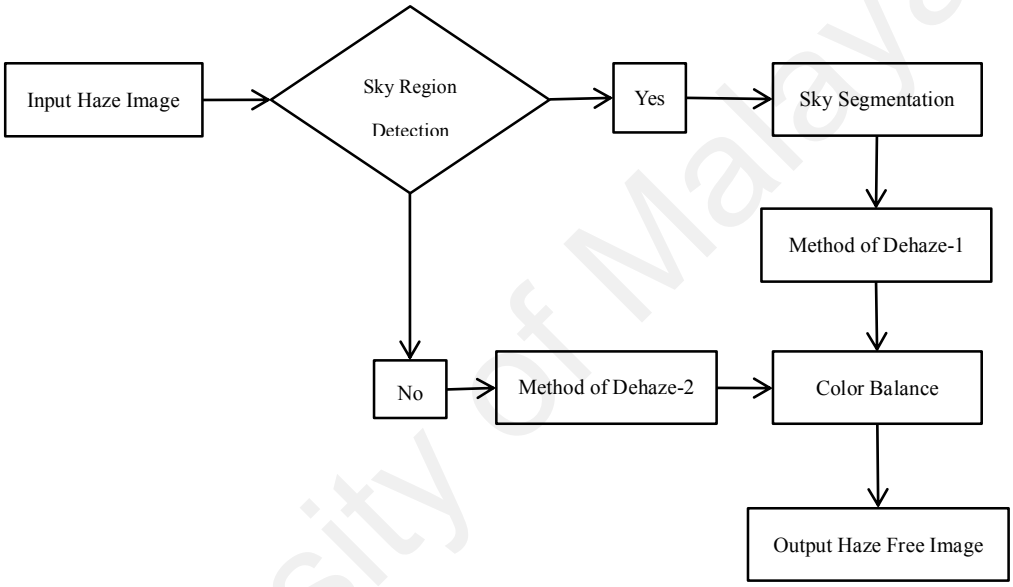

Figure 3.5: The proposed haze removal method

3.4 Design and Implementation

3.4.1 Sky Region Detection and Segmentation

In the haze removal algorithm process of the dark channel prior, this prior law is not applicable in the sky region of the haze image, and the transmittance estimation in the sky region is not accurate and will be smaller than the actual value. This will result in

significant noise amplification and color distortion in the restored dehazing image of the sky region. Although simply setting the global transmittance can improve the visual effect of the image after haze removal to a certain extent, but the change is not obvious and also affects the effect of haze removal of the entire haze image (Mao Tianyi. 2017).

Therefore, in order to obtain the effect of haze removal on the part of the sky region with good visual effects without affecting the overall haze removal, the sky region should be separated for transmittance correction. Aiming at this problem, this research proposed a sky region detection and segmentation algorithm based on the combination of gradient information and brightness threshold. Afterwards, the transmittance of haze images with and without sky regions was corrected.

For the sky region detection and segmentation, the method can be described as follows (Figure 3.6):

i. Input the haze image.
ii. Get the gradient information that used Canny edge detection in the input image.
iii. Label the connection region.
iv. Find the sky region according to the characteristic of brightness of gray scale in the connection region.
v. Segment the sky and the non-sky region.

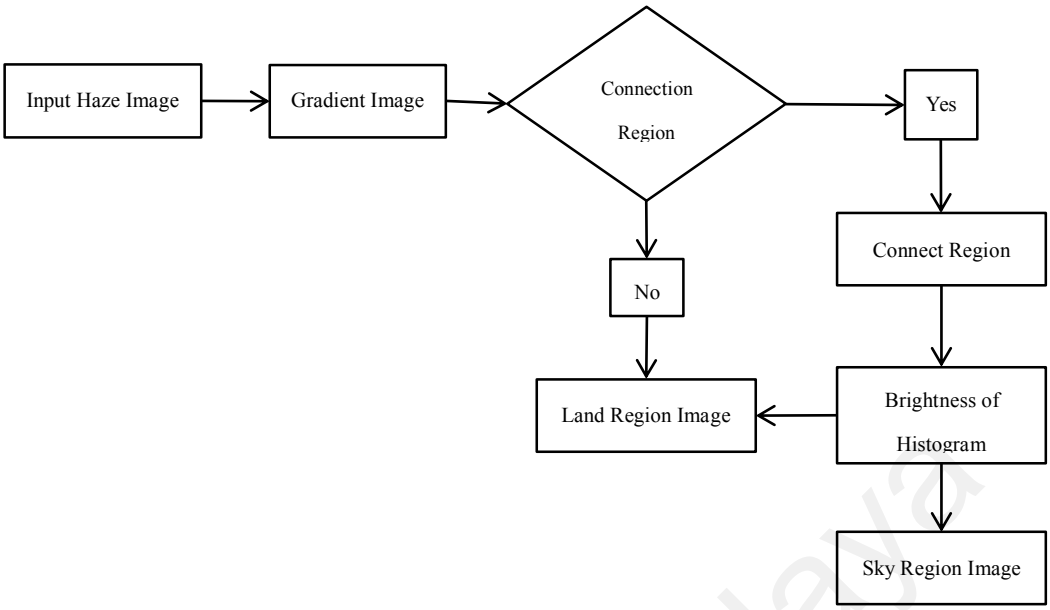

Figure 3.6: The method of sky region segmentation

Step 1: Compute the gradient of each pixel in the input image to get a gradient image. Because the whole sky is smooth, which means there is little change between the adjacent pixels of the image. Therefore, it is easier to identify sky regions by using gradient information. Canny algorithm has been applied in this research.

For the gradient, the function *(z = f(x, y))* has a first order continuous partial derivative in the plane region *(D)*, so for each point *P(x, y)* of the plane region, a vector can be determined

$$\frac{\partial f}{\partial x}\vec{\imath} + \frac{\partial f}{\partial y}\vec{j} \tag{3.1}$$

This vector is called the gradient of the function *(z = f(x, y))* at point *P*

$$gradf(x,y) = \frac{\partial f}{\partial x}\vec{\imath} + \frac{\partial f}{\partial y}\vec{j} \tag{3.1}$$

In the image, set G_x and G_y as the gradient in the x direction and y direction respectively, and the vector of this gradient can be expressed as

$$\nabla f(x,y) = [G_x, G_y]^T = [\frac{\partial f}{\partial x} + \frac{\partial f}{\partial y}]^T \tag{3.2}$$

The amplitude of this vector is

$$mag(\nabla f) = g(x,y) = \sqrt{\frac{\partial^2 f}{\partial x^2} + \frac{\partial^2 f}{\partial y^2}} \quad (3.3)$$

The direction angle can be expressed as follows:

$$\emptyset(x,y) = arctan\left|\frac{\partial f}{\partial y} / \frac{\partial f}{\partial x}\right| \quad (3.4)$$

So in the digital image, the simplest gradient expression is shown below:

$$G_y = f(x,y) - f(x-1,y) \quad (3.5)$$

$$G_y = f(x,y) - f(x,y-1) \quad (3.6)$$

When there are edges in the image, there must be a large gradient value. On the contrary, when there is a smooth part in the image, the changes of gray information is small, and the corresponding gradient value is also small. In this research, the Canny edge detection operator will be used to detect the gradient change of the input image. In image edge detection, both noise suppression and edge accurate positioning cannot be satisfied at the same time. Some edge detection algorithms not only remove noise by smoothing filter, but also increase the uncertainty of edge location. The sensitivity of edge detection operator to edge and the sensitivity to noise are both improved. The Canny operator tried to find the compromise between anti-noise and precise location.

The basic idea of Canny edge detection algorithm is to firstly select a certain Gauss Filter for image smoothing and then use the non-extreme suppression technique to process, and finally get the edge image. The steps are shown as follows:

i. Smooth the image with Gaussian Filter.

The following Gaussian function *(H(x, y))* is used in this research

$$H(x,y) = exp(-\frac{x^2+y^2}{2\sigma^2}) \quad (3.7)$$

$$G(x,y) = f(x,y) * H(x,y) \quad (3.8)$$

where, *f(x, y)* is the data of image.

ii. The amplitude and direction of the gradient are calculated by the finite difference of first order partial derivatives.

Use a first order differential convolution temple

$$H_1 = \begin{vmatrix} -1 & -1 \\ 1 & 1 \end{vmatrix} \qquad H_1 = \begin{vmatrix} 1 & -1 \\ 1 & -1 \end{vmatrix} \tag{3.9}$$

$$\varphi_1(x,y) = f(x,y) * H_1(x,y) \qquad \varphi_2(x,y) = f(x,y) * H_2(x,y) \tag{3.10}$$

Get the amplitude

$$\varphi(x,y) = \sqrt{\varphi_1^2(x,y) + \varphi_2^2(x,y)} \tag{3.11}$$

Direction

$$\theta_\varphi = tan^{-1} \frac{\varphi_2(x,y)}{\varphi_1(x,y)} \tag{3.12}$$

The gradient amplitude is non-maximal suppressed.

The global gradient alone is not enough to determine the edge. In order to determine the edge, the point with the maximum in local gradient must be retained, while the non-maximum value is suppressed. That is to set the non-local maximum point to zero to get a thin edge.

Double threshold algorithm is used to detect and connect the edge.

Using two thresholds T_1 and T_2, two thresholds edge images ($N_1[i,j]$and $N_2[i,j]$) can be obtained. Since $N_2[i,j]$ is worthy of using high threshold, it contains very few false edges, but with discontinuities. The double threshold method is used to connect the edge to the contour in $N_2[i,j]$. When the end point of the contour is reached, the algorithm will search for the edge continuous to the contour in 8 adjacent points of $N_1[i,j]$. In this way, the algorithm continuously collects the edges in $N_1[i,j]$ until

$N_2[i,j]$ in connected.

Step 2: Transform gradient image into a binary image, whose value is '0' if gradient image is smaller than threshold θ, otherwise the value is '1'. Count the probability of gradient information and select the gradient value with the highest probability as the threshold θ.

Step 3: The maximum connected region of the segmented image is selected as the candidate region of sky. The followings pictures show the edge information of each image and its connected region

(a)

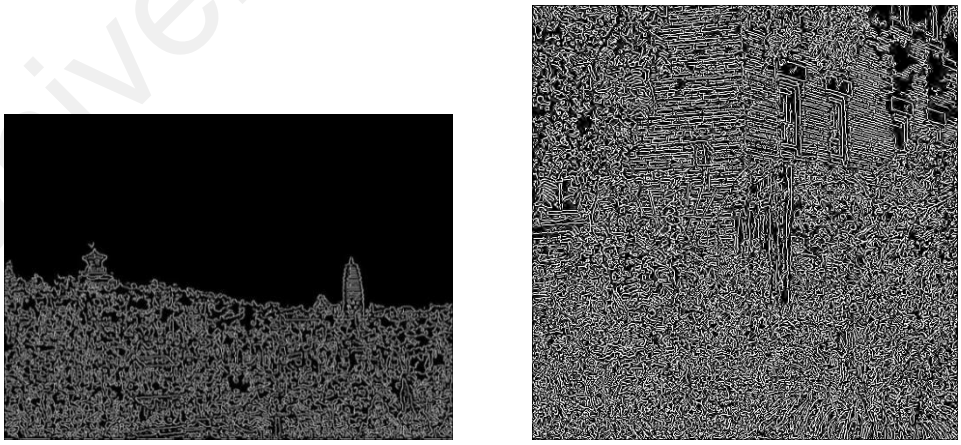

(b)

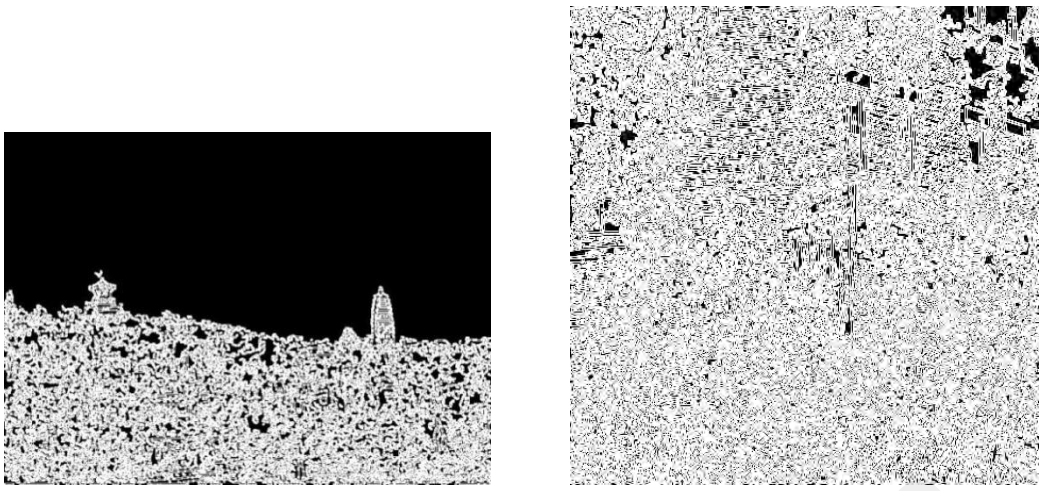

(c)

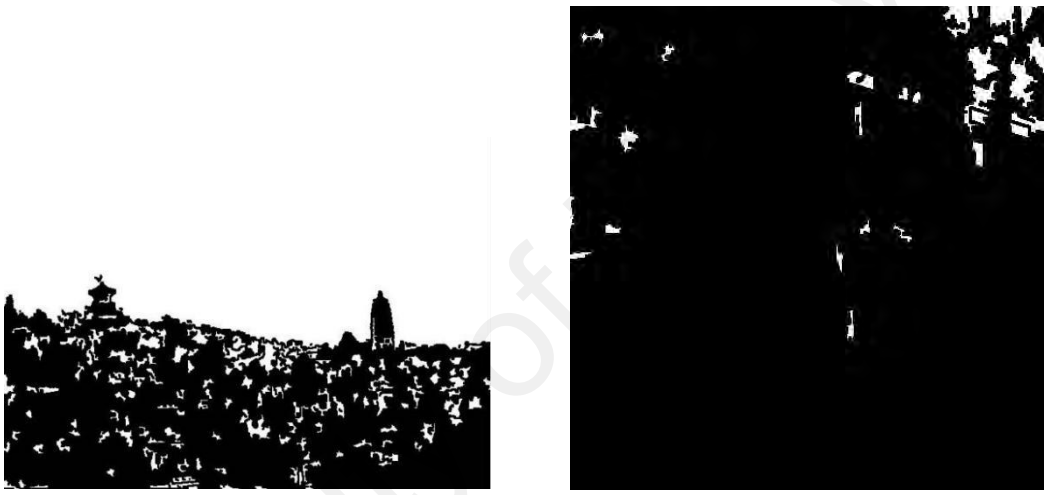

(d)

Figure 3.7: The edge information and its connection region: (a) Haze images, (b) With edge information, (c) Gradient images, (d) Connection regions

Step 4: Direct observation of the image shows that some images with the sky region is more obvious, compared with surrounding scenery that the brightness is generally higher, edge is more clear. However, in some images, the proportion of the sky region is relatively small. This kind of region may has the heavy haze and relatively bright compared with other regions. At this time, it is not regarded as the sky region (Xiao Shengbi & Li Yan, 2015). By analyzing the gray histogram images of haze images

containing the sky region, it was found that images with the sky region showed aggregation on the right side of the histogram image. Some images and their grayscale histogram are shown as in Figure 3.8.

(a)

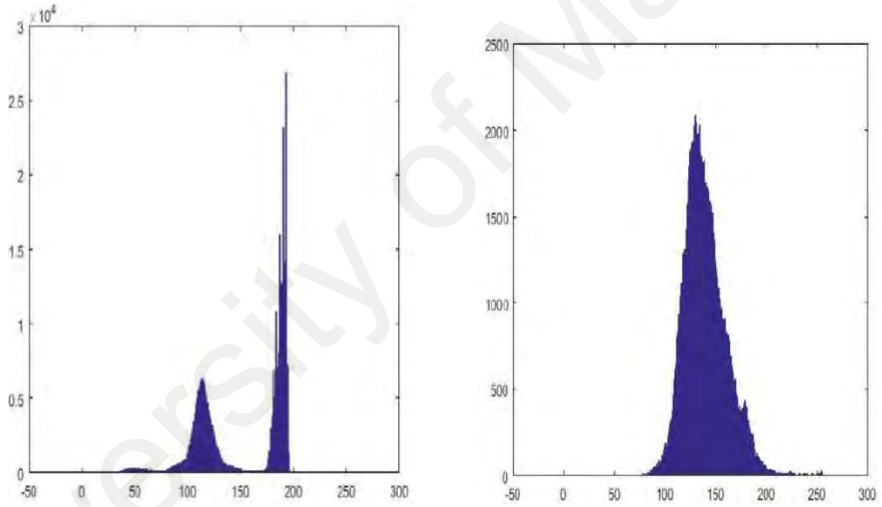

(b)

Figure 3.8: Samples of haze images and its grayscale histogram image: (a) Haze images, (b) Grayscale histogram images

According to the histogram of sky region and non-sky region, the sky region shows aggregation on the right side of the histogram. Although the image of non-sky region also shows aggregation, it is not distributed on the right side. In addition, it can also be clearly seen that there is a certain distance between the aggregation spikes in the sky region image. In other words, there is enough depression between the aggregation

spikes, that is, the proportion of certain pixels is low. So in this step, calculate the brightness histogram of the region, select the threshold of brightness and mark the sky region. Select the brightness threshold by the following steps:

i. Calculate the brightness histogram, mark the mean brightness value as L_{mean}, and mark the max brightness value as L_{max}.

ii. Through many experiments and the selection of different thresholds in this research, finally statistic the maximum frequency of brightness value in the brighter area $[L_{max} - 50, L_{max}]$, and denoted it as L_1.

iii. Statistic the minimum frequency of brightness value between mean value and maximum frequency brightness value $[L_{max}, L_1]$, and denoted it as L_2.

iv. Through many experiments and the selection of different thresholds in this research, finally confirmed $L_3 = (L_1 + L_2)/2$, if $L_{max} - L_3 \geq 30$, the brightness threshold is $L_3 + 40$, if $L_{max} - L_3 \leq 30$, the brightness threshold is $L_3 - 20$, others the brightness threshold is L_3.

The steps are illustrated in Figure 3.9.

(a)

(b)

Figure 3.9: Image of sky segmentation: (a) Haze images, (b) Results after sky segmentation

3.4.2 Method Dehaze-1

For haze images with sky regions, this research optimized the value of transmittance and atmospheric light based on the dark channel dehazing theory, and the specific steps shown in Figure 3.10.

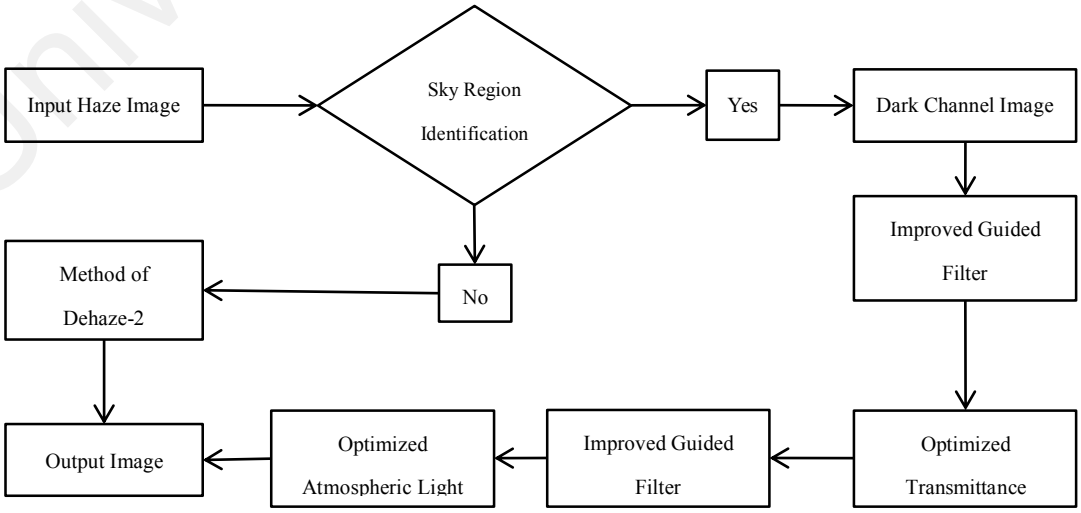

Figure 3.10: The method of Dehaze-1

i. Input the image.

ii. Identify sky region again. (Is the sky region greater than 10% of the total region?)

Since method dehaze-1 will modify the transmittance and the value of atmospheric light according to the sky region, it will become less meaningful when the sky region is too small. Based on the theory and results of the dark channel dehazing method, it is not difficult to find that the color distortion occurs when the image contains large sky region or bright areas. Therefore, it will be verified whether the input image contains sky region or not in this step, so as to eliminate those images without sky region and those with very small sky region. Through a large number of experiments, it is found that the effect is better when the threshold value is 10%.

iii. Get the Dark Channel Image.

In most non-sky local regions, there will always be a phenomenon that there are some very low pixel values in a certain color channel. That is, in haze-free images, it is easy to find very low brightness value points in non-sky region. The formula of dark channel can be described as follows:

$$J^{dark}(x) = \min_{y \in \Omega(x)} (\min_{c \in (r,g,b)} J^c(y)) \rightarrow 0 \quad (3.13)$$

where, $J^c(y)$ refers to the R, G, B channels of image *J(x)*. Firstly, calculate the min value of R, G, B channels in image pixels. Then use minimum filter to process. The min dark channel of haze-free image that without sky region can be described as follows:

$$J^{dark} \rightarrow 0 \quad (3.14)$$

There are three main reasons for the low pixel values in the dark channel mentioned

above. First, the actual scene has shadow under the light, among which buildings, trees and so on will show the dark channel effect in the imaging equipment. Second, the color present in the object is very low in the reflectivity in a certain channel and the dark channel effect can also occur. For example, in green leaves, the green channel is obvious, while red and blue channel are relatively low. Third, the object itself is black or the surface appears black. A haze image and its dark channel image are show in Figure 3.11.

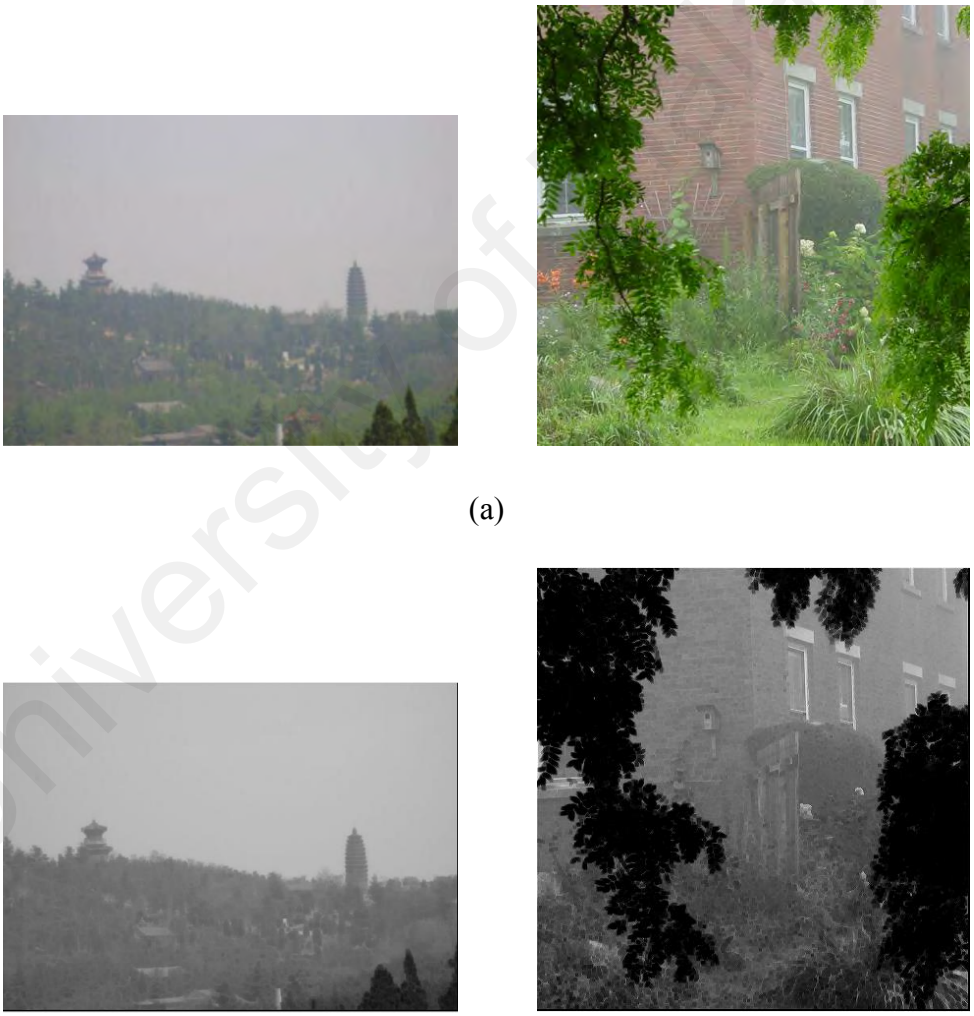

(a)

(b)

Figure 3.11: Haze image and its dark channel image: (a) Haze image, (b) Dark channel image

iv. Use the improved Guided Filter to process.

Assuming that the reference image is *G* and the input image is *I*, where G is the single-channel grayscale of the original image. The filter output $\hat{Z}$ can be regarded as the linear transformation of the reference G under window $W_{\zeta_1}(p)$:

$$\hat{Z}(q) = a_p G(q) + b_p, \forall q \in W_{\zeta_1}(p) \tag{3.15}$$

where, $W_{\zeta_1}(p)$ refers to a square window with a center of p and radius of ζ_1. a_p and b_p are the two constants in the window $W_{\zeta_1}(p)$. q is a field point with the center window of point *p*.

Structure the energy function:

$$E = \sum_{q \in W_{\zeta_1}(p)} [a_p G(q) + b_p - I(p)^2 + \lambda a_p^2] \tag{3.16}$$

where, λ refers to a regularization parameter.

The optimal a_p and b_p can be obtained by the energy function of minimizing

$$a_p = \frac{\mu_{G \cdot I,\zeta_1}(p) - \mu_{G,\zeta_1}(p)\mu_{I,\zeta_1}(p)}{\sigma^2_{G,\zeta_1}(p) + \lambda} \tag{3.17}$$

where, $G \cdot I$ represents the multiplication of the elements of the two matrices, $\mu_{G,\zeta_1}(p)$, $\mu_{I,\zeta_1}(p)$ and $\mu_{G \cdot I,\zeta_1}(p)$ are the average values of G、I and $G \cdot I$.

The final output of the filter is

$$\hat{Z}(p) = \bar{a}_p G(p) + \bar{b}_p \tag{3.18}$$

where, $\bar{a}_p$ and $\bar{b}_p$ represent the average values of a_p and b_p in $W_{\zeta_1}(p)$.

At this point, in order to get better edge retention characteristics, a constraint term η_p and edge retention term $\Gamma_G(p)$ are introduced, and the improved energy function is

$$E = \sum_{q \in W_{\zeta_1}(p)} [a_p G(q) + b_p - I(p)^2 + \frac{\lambda}{\Gamma_G(p)}] \tag{3.19}$$

The optimal a_p and b_p are obtained

$$a_p = \frac{\mu_{G\cdot I,\zeta_1}(p) - \mu_{G,\zeta_1}(p)\mu_{I,\zeta_1}(p) + \frac{\lambda}{\Gamma_G(p)}\eta_p}{\sigma^2_{G,\zeta_1}(p) + \frac{\lambda}{\Gamma_G(p)}} \tag{3.20}$$

$$b_p = \mu_{I,\zeta_1}(p) - a_p\mu_{G,\zeta_1}(p) \tag{3.21}$$

$\Gamma_G(p)$ is defined as

$$\Gamma_G(p) = \Gamma_{1G}(p)\Gamma_{2G}(p) \tag{3.22}$$

$$\Gamma_{1G}(p) = \frac{1}{N}\sum_{q=1}^{N} \frac{\sigma^2_{G,\zeta_1}(p) + \varepsilon}{\sigma^2_{G,\zeta_1}(q) + \varepsilon} \tag{3.23}$$

$$\Gamma_{2G}(p) = [\left(\frac{\partial Z(p)}{\partial x}\right)^2_{sobel} + \left(\frac{\partial Z(p)}{\partial y}\right)^2_{sobel}]^{-1} \tag{3.24}$$

where, $Z(p)$ is the output value of point p in the filter, ε is a constant value, η_p is used to ensure that the improved guided filter performs better filtering in smooth areas while maintaining good edge properties.

$$\eta_p = [1 + exp\left(k_p \frac{\mu_\sigma^2 - \sigma^2_{G,\zeta_1}(p)}{\mu_\sigma^2 - min\left(\sigma^2_{G,\zeta_1}(q)\right)}\right)]^{-1} \tag{3.25}$$

where, μ_σ^2 refers to the average value of variance of image gray value $\sigma^2_{G,\zeta_1}(p)$ in window $W_{\zeta_1}(p)$.

Set *I*=*G*, and if p is in the smooth region, then $\eta_p \approx 0$, and a_p can expressed as follows:

$$a_p = \frac{\sigma^2_{G,\zeta_1}(p)}{\sigma^2_{G,\zeta_1}(p) + \frac{\lambda}{\Gamma_G(p)}} \tag{3.26}$$

If p is near the edge, then $\eta_p \approx 1$, and a_p can expressed as follows:

$$a_p = \frac{\sigma^2_{G,\zeta_1}(p) + \frac{\lambda}{\Gamma_G(p)}}{\sigma^2_{G,\zeta_1}(p) + \frac{\lambda}{\Gamma_G(p)}} = 1 \tag{3.27}$$

At this point, the gradient value of the filter output image is equal to the gradient value of the input image, which means the edge of the original image is well preserved.

Therefore, the improved guided filter can achieve a good smooth filter in the smooth region, and retain the edge characteristics of the original image.

The Figure 3.12 shows the dark channel image processed with the improved guided filter.

(a) (b)

Figure 3.12: Image after using Guided Filter: (a) Dark channel image, (b) Improved guided filter

v. Optimize the transmittance of the image.

The estimation of transmittance is an important part of the algorithm. The accurate transmittance is obtained, which means that the final dehazing effect is improved. According to the dark channel theory, in any color channel c(R, G, B):

$$I^c(x) = J^c(x)t(x) + A^c(1 - t(x)) \tag{3.28}$$

where, I is the haze image, J is the haze-free image, A is the global atmospheric light, in general, it is assumed to be global, irrespective of local location x. t is the transmittance.

Assume that atmospheric light values are globally constant, after normalization:

$$\frac{I^c(x)}{A^c} = t(x)\frac{J^c(x)}{A^c} + 1 - t(x) \tag{3.29}$$

Then perform twice minimum operations on both sides of the formula:

$$\min_{y\epsilon\,\Omega\,(x)}(\min_{A^c}\frac{I^c(y)}{A^c}) = t(x)\min_{y\epsilon\Omega(x)}(\min_{A^c}\frac{J^c(y)}{A^c}) + 1 - t(x) \quad (3.30)$$

Based on the dark channel theory, for some pixels in a local area of the non-sky part of the natural image, at least one color channel has a very low brightness value and it approaches 0.

$$J_{dark}(x) = \min_{c\in(r,g,b)}(\min_{y\epsilon\Omega(x)}(J^c(y))) \to 0 \quad (3.31)$$

where

$$\min_{y\epsilon\Omega(x)}(\min_{c}\frac{I^c(y)}{A^c})) \quad (3.32)$$

The formula for calculating the transmittance can be described as follows:

$$t(x) = 1 - \min_{c\in(r,g,b)}(\min_{y\epsilon\Omega(x)}\left(\frac{I^c(y)}{A^c}\right)) \quad (3.33)$$

In order to restore the image to maintain a certain level of sense, it is necessary to preset a haze retention factor $\omega(0 \le \omega \le 1)$. So the formula for calculating the normal transmittance can be described as follows:

$$t(x) = 1 - \omega\min_{c\in(r,g,b)}(\min_{y\epsilon\Omega(x)}\left(\frac{I^c(y)}{A^c}\right)) \quad (3.34)$$

However, in general, the transmittance value estimated by using dark channel prior algorithm in haze images with sky region is generally small to different degrees. Therefore, this section will optimize the transmittance of haze images with sky region. In the previous section, the sky region in the haze image has been segmented. The segmented binary image is converted into gray scale image and processed with the mean filter. Mean filter is also called linear filter. The main method is neighborhood average. The basic principle of linear filter is used the average value instead of the value in each pixel of original image. That is to choose a template to deal with the

current pixel point *(x, y)*, this template is composed of the neighbor number of pixels, and calculate the average of all pixels in the temple. Then gives the mean value to the current pixel point *(x, y)*, as a gray scale value g in point *(x, y)*.

$$g(x,y) = {}^{1}/_{m} \sum f(x,y) \tag{3.35}$$

where, *m* refers to the number of pixels in the template

The binary image of sky region and its gray image after using mean filter are shown in Figure 3.13.

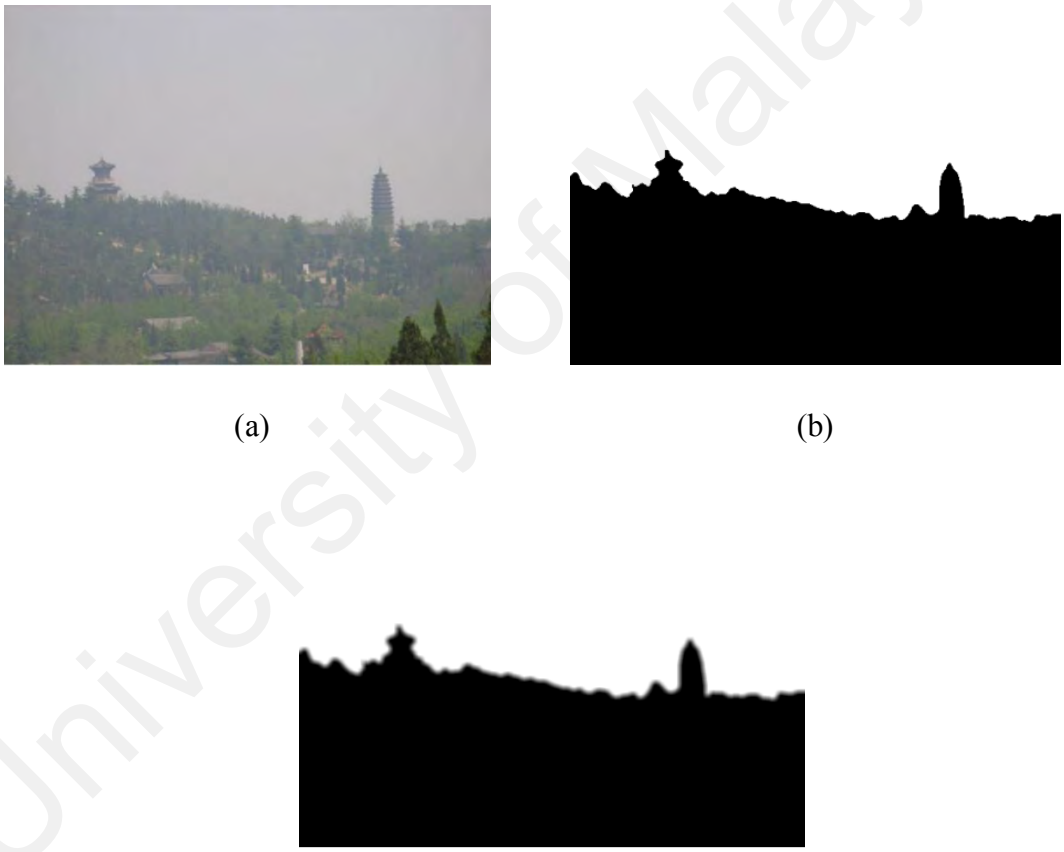

(a) (b)

(c)

Figure 3.13: Image after using mean filter: (a) Haze image, (b) Binary image, (c) Gray image after using mean filter

Set I_{sky} is the value of image c, so the value of I_{sky} is 0 in the non-sky region, the value of I_{sky} is 255 in the sky region, and the value of I_{sky} is between 0 to 255 at the

junction of the sky region and non-sky region.

After obtaining the value of I_{sky}, the formula of optimized transmittance is shows as follows:

$$J(t) = 1 - \omega * \frac{(15 * I_{sky} + \omega * J_{dark} * (255 - I_{sky}))}{255} \quad (3.36)$$

where, J_{dark} is the input dark channel image, I_{sky} is the value of gray scale image of the binary of sky region image, $I_{sky} \in (0,255)$. Among them, the best effect can be obtained when ω is 0.75 through lots of experiments. The estimation of transmittance is illustrated in Figure 3.14.

(a) (b)

Figure 3.14: Transmittance image: (a) Haze image, (b) Transmittance image

vi. Use the Improved Guided Filter to process.

Improved Guided Filter is used again to process the obtained transmittance image, and the estimation of result is demonstrated in Figure 3.15.

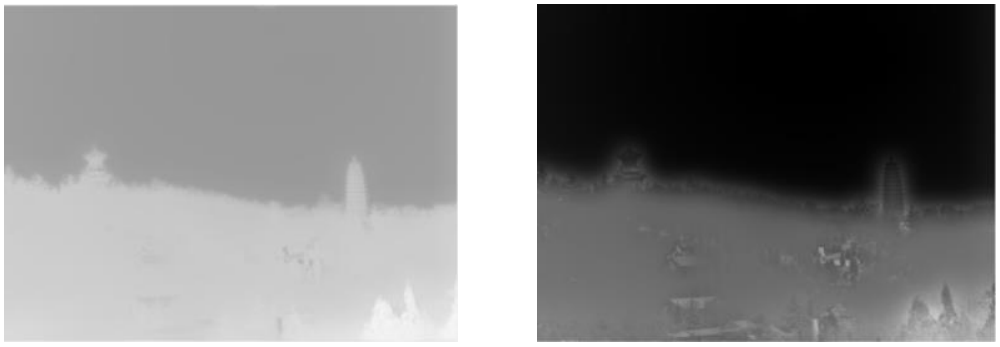

(a) (b)

Figure 3.15: The image after using Guided Filter: (a) Transmittance image, (b) Transmittance image after filtering

vii. Optimize the value of atmospheric light.

According to the parameters in the formula (2.23) of haze image restoration, it can be found that in addition to the estimation of transmittance, the acquisition of atmospheric light value is also very important. If the atmospheric light value is not accurate, it will have a great impact on the overall effect of haze removal. Figure 3.16 shows the effect of different atmospheric light values on the results.

(a) (b) (c)

Figure 3.16: The effect of different atmospheric light: (a) Haze image, (b) Result of inaccurate estimate of atmospheric light, (c) Result of accurate of atmospheric light

Atmospheric light means ambient light at an infinite distance from the imaging

equipment. In other words, if there is a large clear sky region, the value of atmospheric light should be in the sky region. If there is no obvious sky region, atmospheric light should be in the area with the densest haze. And the estimation of incorrect atmospheric light position is illustrated in Figure 3.17. The red box indicates the wrong position of atmospheric light.

Figure 3.17: The wrong atmospheric position in haze images

Therefore, for haze images with large brightness or sky regions, it is not advisable to calculate atmospheric light value in the haze removal algorithm based on dark channel prior. In this section, the average brightness value of the sky region is used to replace the way to calculate atmospheric light value in dark channel prior algorithm,

which can effectively avoid the problem of color distortion in the sky region after dehazing.

viii. Image dehazing and output image.

Finally, the parameters of transmittance and atmospheric light value are modified, and the filter is optimized. For haze images with sky and large brightness regions, the effect of haze removal is shows in Figure 3.18.

(a)

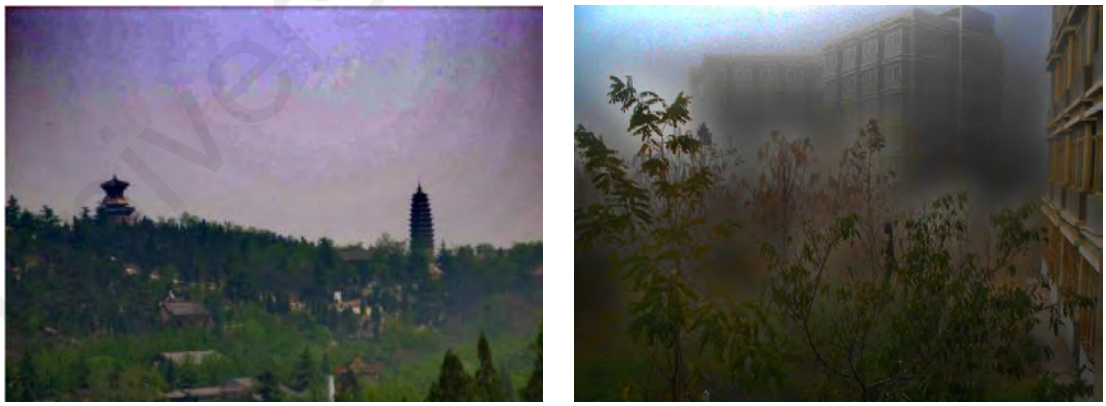

(b)

(c)

Figure 3.18: Effect of haze removal: (a) Haze images, (b) Haze free images after using DCP, (c) Haze free images after using proposed method

3.4.3 Method Dehaze-2

For haze images without sky regions, in this research, bilateral filter was used to replace the guided filter that used in the haze removal algorithm based on dark channel prior, and inverse filter was applied to the transmittance image. The results showed that the modified method had a good processing effect on the haze images, and the specific steps are show in Figure 3.19.

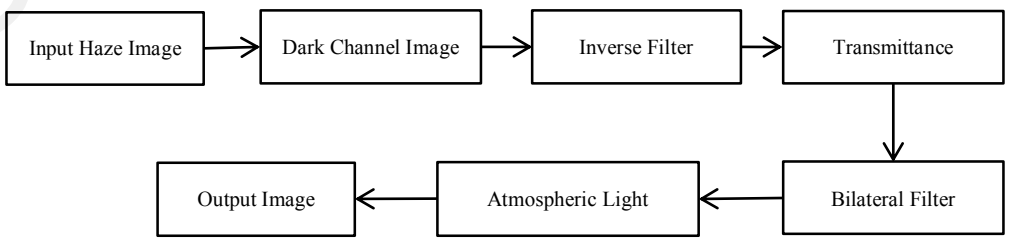

Figure 3.19: The method of Dehaze-2

i. Input the image.

ii. Get the Dark Channel Image.

For the input haze image without large sky region, the method of obtaining the dark channel image in method of dehaze-1 is used in this section. And the estimation of dark channel image is demonstrated in Figure 3.20.

(a)

(b)

Figure 3.20: Estimation of dark channel: (a) Haze images, (b) Dark channel images

iii. Use the Inverse Filter to process

In the process of collection, transmission and preservation, the image is often affected by various factors, such as channel interference and the loss of image information. Under the influence of these factors, the image will degrade to some extent. Image restoration method is to use some knowledge of degradation features to reconstruct the degraded image. The image restoration method by degradation function is inverse filtering. Let's say the Fourier transform before the degradation is *F(x, y)*, the Fourier transform after the degradation is *G(x, y)*, the Fourier transform of degradation function is *H(x, y)*. Inverse filter is the Fourier transform of degradation function divided by the degraded image. Then the estimated value of the Fourier transform of the degraded image is obtained, where *N(x, y)* is the Fourier transform of noise.

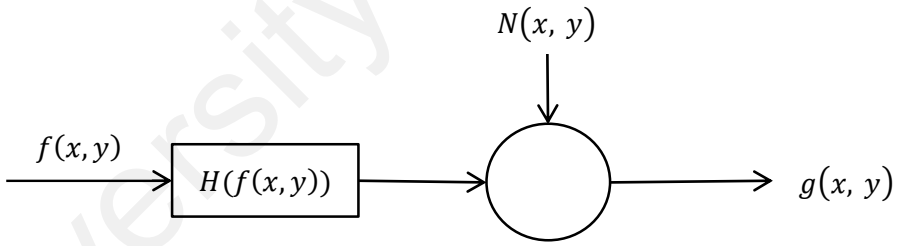

Figure 3.21: General mathematical model of image degradation

The original image $f(x,y)$ is processed by an image degradation restoration system $H(x,y)$, and then overlapped with noise $N(x,y)$ to obtain the degraded image $g(x,y)$ as shown in Figure 3.21.

The mathematical expression for $g(x,y)$ is

$$g(x,y) = H[f(x,y)] + N(x,y) \tag{3.37}$$

where, $H[\cdot]$ is the function of prior information (degradation model).

When $H[\cdot]$ is a linear operator:

$$H\big(k_1 f_1(x,y)\big) + H\big(k_2 f_2(x,y)\big) = k_1 H\big(f_1(x,y)\big) + k_2 H\big(f_2(x,y)\big) \quad (3.38)$$

where, k_1 and k_2 are constants:

$$H\big(f(x,y)\big) = H\Big(\int_{-\infty}^{\infty}\int_{-\infty}^{\infty} f(\alpha,\beta)\delta(x-\alpha,y-\beta)d_\alpha d_\beta\Big) = \int_{-\infty}^{\infty}\int_{-\infty}^{\infty} H\big(f(\alpha,\beta)\delta(x-\alpha,y-\beta)d_\alpha d_\beta\big) = \int_{-\infty}^{\infty}\int_{-\infty}^{\infty} f(\alpha,\beta)h(x,y:\alpha,\beta)d_\alpha d_\beta \quad (3.39)$$

where, $h(x,y:\alpha,\beta) = H(f(\alpha,\beta)\delta(x-\alpha,y-\beta))$ is shock response of $H(x,y)$. $h(x,y:\alpha,\beta)$ is point spread function (PSF) in degradation process.

Set $H(x,y)$ is time shift invariant, that $H[\cdot]$ satisfies $h(x,y:\alpha,\beta) = g(x,y:\alpha,\beta)$:

$$g(x,y) = \int_{-\infty}^{\infty}\int_{-\infty}^{\infty} f(\alpha,\beta)h(x-\alpha,y-\beta)d_\alpha d_\beta) + N(x,y) = f(x,y)h(x,y) + N(x,y) \quad (3.40)$$

In fact, $g(x,y)$ is the known quantity, and $h(x,y)$ and $N(x,y)$ can be used as the prior information, finally get $f(x,y)$.

The formula (3.40) is discretized:

$$g = Hf + N \quad (3.41)$$

Which is expressed as a two-dimensional image matrix, and 3.42 can be obtained:

$$G(u,v) = T \cdot M \cdot E(u,v) + N(u,v) \quad (3.42)$$

where, $M = A + C - 1, T = B + D - 1$, *A, B, C, D* are the dimensions of $f(x,y)$ and $h(x,y)$.

The noise term $(N = g - Hf)$ can be obtained by deformation of formula 3.41. The image restoration is no noise, that is, $N(x,y)$ goes to 0. Then a certain criterion is

taken to look for f

$$J(\hat{f}) = ||g - H\hat{f}||^2 = ||N||^2 \tag{3.43}$$

$$||N||^2 = N^T N, \qquad ||g - Hf||^2 = \left(g - H\hat{f}\right)^T (g - H\hat{f}) \tag{3.44}$$

It can be obtained from the extremum condition:

$$\frac{\partial ||n||^2}{\partial \hat{f}} = 0 \Rightarrow H^T\left(g - H\hat{f}\right) = 0 \Rightarrow \hat{f} = H^{-1}(H^{-1})^2 H^T g \tag{3.45}$$

where, when $M=T$, sets H^{-1} exists:

$$\hat{f} = H^{-1}(H^{-1})^2 H^T g = H^{-1} g \tag{3.46}$$

Since H is a block circular matrix, it can be proved that H can be diagonalized, i.e:

$$H = WDW^{-1} \tag{3.47}$$

where, the size of W are $MT*MT$, so there is

$$\hat{f} = (WDW^{-1})^{-1} g = (WD^{-1}W^{-1})g \Rightarrow W^{-1}\hat{f} = D^{-1}W^{-1}g \tag{3.48}$$

the following formula is further obtained:

$$\hat{F}(u,v) = \frac{G(u,v)}{N^2 H(u,v)} \tag{3.49}$$

Finally $F(u,v)$ is got by the formula 3.49, and $f(x,y)$ is got by the inverse Fourier transform. The inverse filter images are shown in Figure 3.22.

(a)

(b)

Figure 3.22: The inverse filter images: (a) Dark channel images, (b) Inverse filter images

iv. Get the transmittance image.

The estimation of transmittance in this section uses the calculation formula of formula (3.34) in method of dehaze-1. For the method of dehaze-2 in this research, ω

is 0.95. The formula of transmittance can be described as follows:

$$J(t) = 1 - \omega * J_{dark} \tag{3.50}$$

where, J(t) is the transmittance, J_{dark} is the dark channel image.

v. Use Bilateral Filter to process.

Bilateral filter is a non-linear smoothing filter for image, which preserves the edge and reduces the noise of images. In this research, through experimental comparison, it is found that bilateral filter is better than guided filter in the effect of haze image processing, although it is at a disadvantage in processing speed. In method of Dehaze-2, there is no complicated process, and better results can be achieved by using bilateral filter. It uses the weighted average of intensity values of nearby pixels to take the place of the intensity value of each pixel. The bilateral filter is defined as:

$$I_{filtered}(x) = \frac{1}{W_p}\sum_{x_i \in \Omega} I(x_i) f_r(\left|\left|I(x_i) - I(x)\right|\right) g_s(\left|\left|x_i - x\right|\right|) \tag{3.51}$$

where, the normalization term

$$W_p = \sum_{x_i \in \Omega} f_r\left(\left|\left|I(x_i) - I(x)\right|\right) g_s(\left|\left|x_i - x\right|\right|) \tag{3.52}$$

Ensure that the filter preserves image energy and:

$I_{filtered}$ is the filtered image;

I refers to the original input image which is to be filtered;

X is the coordinates of the present pixel to be filtered;

Ω refers to the window centered in x;

f_r refers to the range kernel for smoothing differences in intensities;

g_s refers to the spatial kernel for smoothing differences in coordinates;

As is indicated above, the weight W_p is assigned using the spatial closeness and the intensity difference. Consider a pixel located at (*i, j*) that needs to be denoised in image using its neighbouring pixels and one of its neighbouring pixels is located at (*k, l*). Then, the weight assigned for pixel (*k, l*) to denoise the pixel (*i, j*) is given by

$$\omega(i,j,k,l) = exp(-\frac{(i-k)^2+(i-l)^2}{2\sigma_d^2} - \frac{||I(i,j)-I(k,l)||^2}{2\sigma_r^2}) \quad (3.53)$$

where $\sigma_d$and σ_r refer to smoothing parameters, and *I*(*i* , *j*) and *I*(*k* , *l*) are the intensity of pixels (*i, j*) and (*k, l*) respectively.

After the weights are calculated, normalize them

$$I_D(i,j) = \frac{\sum_{k,l} I(k,l)\omega(i,j,k,l)}{\sum_{k,l}\omega(i,j,k,l)} \quad (3.54)$$

where, I_D refers to the denoised intensity of pixel (*I, j*).

After using Bilateral Filter to processed, the results are shown in Figure 3.23.

Figure 3.23: The bilateral filter images

vi. Get the value of atmospheric light of the image.

When estimating the atmospheric light, the value of maximum brightness points of the input image is used as the value of atmospheric light in dark channel prior

algorithm. The specific method is divided into two steps:

1. Sort by the brightness in the dark channel image, take the value of first 0.1%.
2. Locate the brightness value obtained to the position in accord with the original image. Find the maximum of these positions as the value of atmospheric light.

vii. Image dehazing and output image.

For haze images without sky and large brightness regions, the effect of haze removal are shown in Figure 3.24.

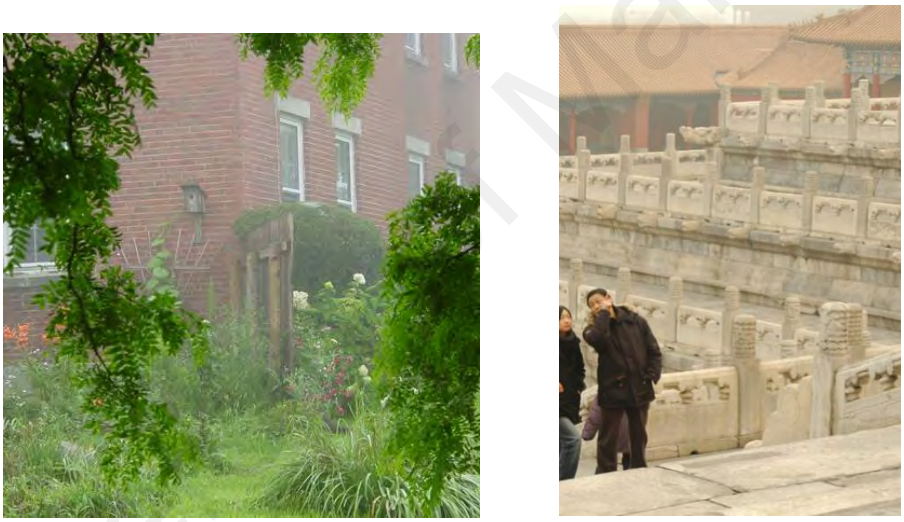

(a)

(b)

(c)

Figure 3.24: Effect of haze removal: (a) Haze images, (b) Haze free images after using DCP, (c) Haze free images after using proposed method

3.4.4 Color Balance

When a color image is digitized, it often looks a little out of whack. This is due to the different sensitivity of the color channel, the enhancement factor and the offset, and it is called the tricolor imbalance. The color balance algorithm consists of the following three steps.

i. Select two points color from the screen as gray.

$$F_1 = (R_1, G_1, B_1) \tag{3.55}$$

$$F_2 = (R_2, G_2, B_2) \tag{3.56}$$

ii. Set the G component as reference, and match the R and B components.

$$F_1 = (R_1, G_1, B_1) \Rightarrow \quad F_1^* = (R_1, G_1, B_1) \tag{3.57}$$

$$F_2 = (R_2, G_2, B_2) \Rightarrow \quad F_2^* = (R_2, G_2, B_2) \tag{3.58}$$

iii. Figure out k1 and k2 from $R_1^* = k1 * R_1 + k2$ and $R_2^* = k1 * R_2 + k2$, and figure out l1 and l2 from $B_1^* = l1 * B_1 + l2$ and $B_2^* = l1 * B_2 + l2$.

iv. use

$$R(x,y)^* = k1 * R(x,y) + k2 \tag{3.59}$$

$$B(x,y)^* = l1 * B(x,y) + l2 \tag{3.60}$$

$$G(x,y)^* = G(x,y) \tag{3.61}$$

The processed image is the image after color balance. The effect of color balance is shown as in Figure 3.25.

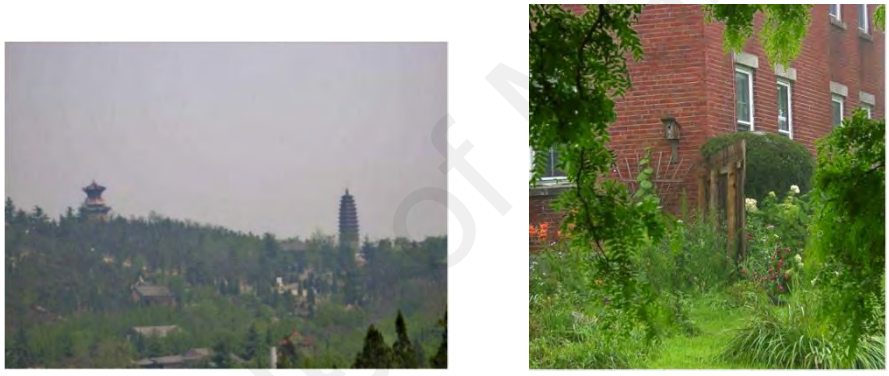

(a)

(b)

Figure 3.25: The effect after color balance: (a) Haze free images, (b) Results after color balance

3.5 Summary

Research methodology of the proposed method is briefly described in this whole chapter. Full research methodology is explained into two phases. In the first phase, requirement analysis has been described and in the second phase, explanation of research design and implementation has been given in procedural steps. The proposed method in this chapter mainly consists of two parts, which are respectively used for haze image with sky region and those without sky region. In addition, the effect of the proposed method in this chapter is compared with that of the haze removal algorithm based on dark channel prior. From the subjective evaluation of the naked eye, the proposed method in this chapter has better results. More evaluation methods will be detailed in chapter 4.

CHAPTER 4

EXPERIMENTAL RESULTS AND EVALUATION

4.1 Introduction

In this chapter, through the proposed method in Chapter 3, different types of images in the dataset are processed separately. At the same time, in this chapter, the results of the proposed method will be in comparison with other traditional haze removal algorithms, and the comparison method is subjective and objective. The traditional 4 haze removal algorithms include DCP (He Kaiming, 2011), Fattal (Rannan Fattal, 2008), Retinex and GHH (Global Histogram Homogenization), where the GHH method and Retinex are based on image enhancement. And in this chapter, NIQE (Natural Image Quality Evaluator) is selected as the objective evaluation standard of images.

This chapter is divided into 6 sections. The development environment of this research is mainly introduced in section 4.2. In section 4.3, 4 traditional haze removal algorithms that used to comparison are briefly introduced. In section 4.4, NIQE used for objective evaluation is mainly introduced. In section 4.5, some classic haze images are selected from dataset, respectively processed by the proposed haze removal method and other 4 traditional haze removal algorithms, and the effect of each algorithm is evaluated by using NIQE. And this chapter is mainly summarized in section 4.6.

4.2 Experimental Environment

The proposed research was programmed and simulated using the MATLAB 2016a software (The Math Works, Natick MA, USA). The machine configured with a 2.9 GHz Intel Pentium Core i5-4210H processor and 8GB of RAM and Windows 10 professional 64-bit operating system (Microsoft, Redmond, WA, USA). The experiments are conducted on the dataset from two parts, as described in section 3.21.

4.3 Four Traditional Haze Removal Methods

4.3.1 Haze Removal Based on Dark Channel Prior

This algorithm is based on dark channel prior theory, and the haze image is processed by atmospheric physical scattering model. The detailed steps of this method are explained in chapter 2.

4.3.2 Haze Removal Based on Fattal

This algorithm first assumes that the light is uniform space of all the same types, and the transmittance is not correlated with the local surface projection. Then, it estimates the transmittance of the object, and calculates the transmittance of light through the scattering value which approximates the truth in the process of light transmittance. Finally, remove the haze of image.

4.3.3 Haze Removal Based on Retinex

This algorithm is based on the color constancy theory, that is, the color of object does not depend on the intensity of reflected light, but on the object's ability to reflect the three primary colors of light (Land E H, McCann J J. 1971). In recent years, researchers have looked for ways to remove the haze from haze images.

4.3.4 Haze Removal Based on GHH

The histogram is mainly to compress the gray level with low pixels in the image, and at same time, to widen the gray level with high pixels in the image. The gray histogram of the image is uniformly distributed through nonlinear stretching, so as to improve the contrast and gray change of the haze image, so as to achieve the visual dehaizng effect.

4.4 NIQE Objective Evaluation Criteria

NIQE does not use the distorted image of human eye score for training. After calculating the local MSCN normalized image, part of the image blocks are selected as the training data according to the local activity, and the model parameters obtained by the generalized Gaussian model fitting are used as the characteristics, multivariable Gaussian model is used to describe those characteristics. This method calculates the normalized brightness of the image in firstly. Assuming that the brightness image is *I(i, j)*, the formula for its separation normalization is as follows:

$$I(i,j) = {I(i,j) - u(i,j)}\Big/{\sigma(i,j)} + c \tag{4.1}$$

$$\sigma(i,j) = \sqrt{\sum\sum w_{k,j}(I_{k,j}(i,j) - \mu(i,j))^2} \tag{4.2}$$

$$\mu(i,j) = \sum\sum w_{k,j}\, I_{k,j} \tag{4.3}$$

where, *i* and *j* refer to the spatial coefficient, *c* is a constant, *w* is a Gaussian weight function with circular symmetry.

The image is divided into image blocks *(p*p)*, calculate the local mean variance *(σ)* of the image block *(b)*

$$\sigma(b) = \sum\sum_{(i,j)\in b} \sigma(i,j) \tag{4.4}$$

The normalization coefficient of the characteristic image block is fitted by the GGD (generalized Gaussian distribution) model.

The AGGD (asymmetrical generalized Gaussian distribution) model is used to fit the product of 4 adjacent coefficients.

Then the parameters *v* and $\sum$ are calculated by fitting MVG (Multivariate Gaussian) model, where *v* is the average value and $\sum$ is the variance matrix. MVG model formula is as follows:

$$f_x(x_1, x_2, \dots, x_k) = \frac{1}{2\pi^{k/2}|\sum|^{1/2}} exp(-\frac{1}{2}(x-v)^T \sum^{-1}(x-v)) \tag{4.5}$$

where, $x_1, x_2, \dots, x_k$ is the image features extracted.

The image quality is measured by calculating the distance between the distorted image and the natural image fitting parameters. The specific calculation formula is as follows:

$$D(v_1, v_2, \sum_1, \sum_2) = \sqrt{(v_1 - v_2)^T (\frac{\sum_1 + \sum_2}{2})^{-1}(v_1 - v_2)} \tag{4.6}$$

Finally, a smaller score indicates better perceptual quality (Mittal, et al 2013) .

4.5 Image Dehazing Results Contrast

Figure 4.1 to 4.7 show the outdoor haze removal image produced by five methods including the proposed method.

Table 4.1 to 4.7 illustrate the NIQE results of four traditional haze removal method and the proposed method. The less NIQE value indicates the better result.

In this research, haze images in different scenes were selected for haze removal, these seven images including haze images with sky region, haze image without sky region, and haze images captured by monitoring equipment, etc. And these seven images are quite representative in these three different haze scenes. In terms of subjective evaluation and objective evaluation, the proposed method shows the best result among the four methods for haze removal.

4.5.1 Haze Image with Sky Region

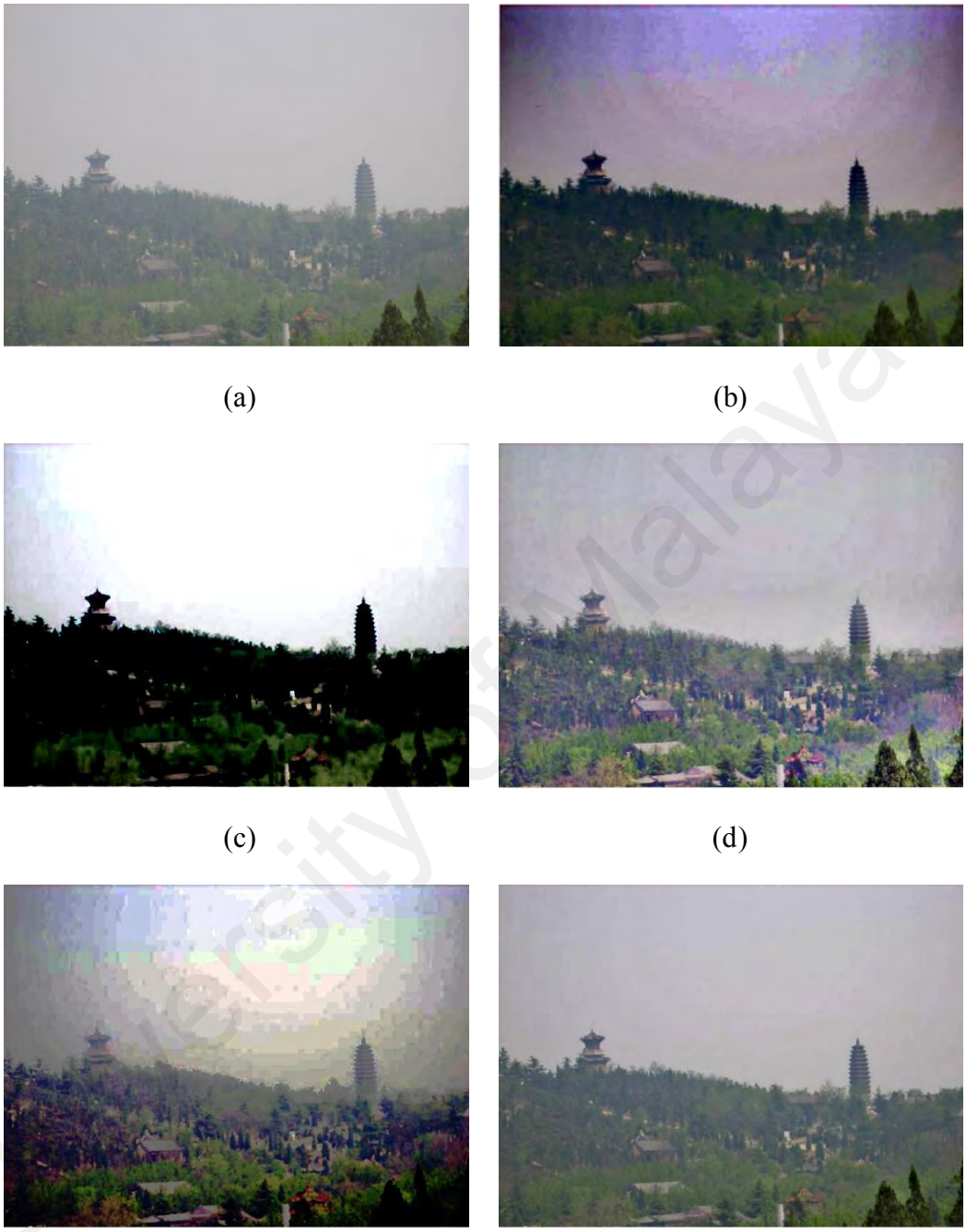

(a) (b)

(c) (d)

(e) (f)

Figure 4.1: The effect of five haze removal methods: (a) Haze image, (b) DCP, (c) Fattal, (d) Retinex, (e) GHH, (f) Proposed method

NIQE quality evaluation score:

Table 4.1: Score of result of each method

	DCP (He K. M., 2011)	**FATTAL (Fattal R., 2008)**	**RETINEX (Fu X et al., 2014)**	**GLOBAL HISTOGRAM HOMOGENIZATION (Sheng H. L., 2015)**	**PROPOSED METHOD**
NIQE	4.7807	7.2982	4.8613	5.7254	4.7561

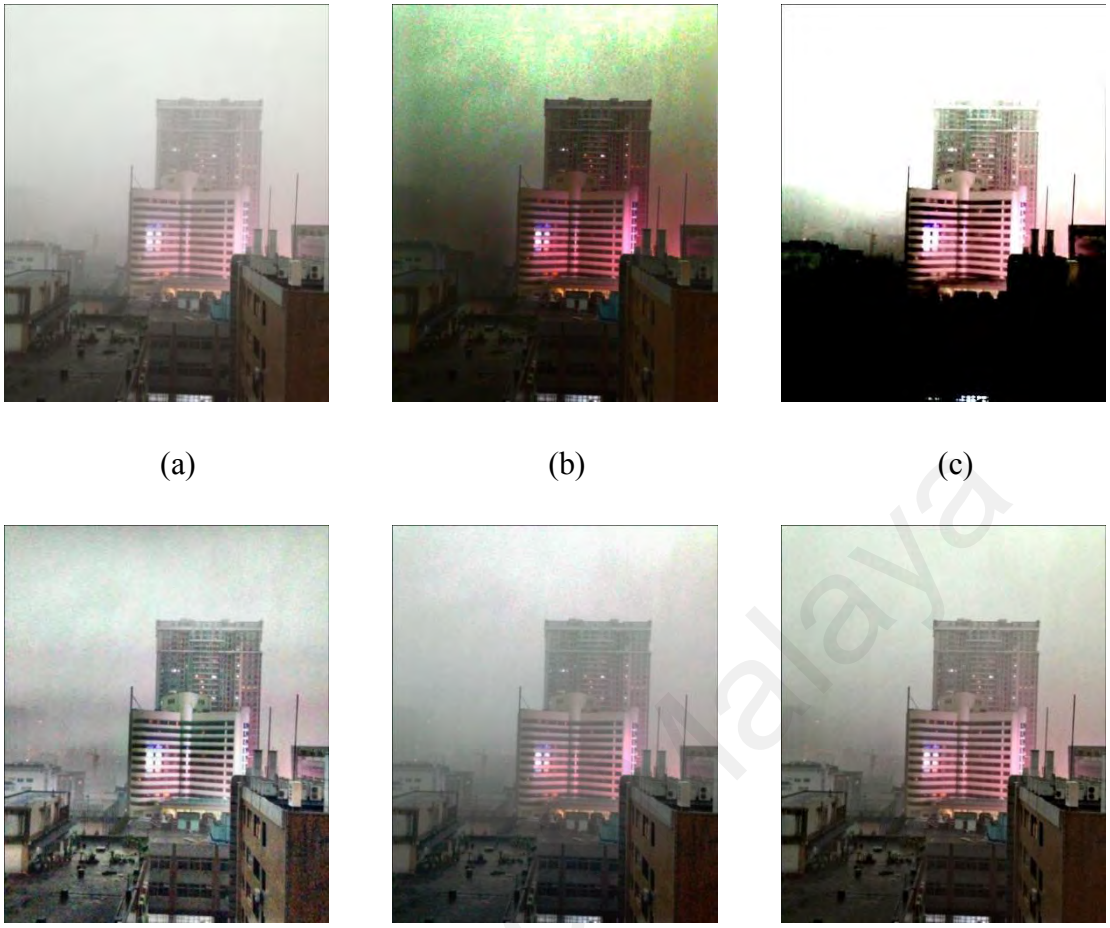

(a) (b) (c)

(d) (e) (f)

Figure 4.2: The effect of five haze removal methods: (a) Haze image, (b) DCP, (c) Fattal, (d) Retinex, (e) GHH, (f) Proposed method

NIQE quality evaluation score:

Table 4.2: Score of result of each method

	DCP (He K. M., 2011)	**FATTAL (Fattal R., 2008)**	**RETINEX (Fu X et al., 2014)**	**GLOBAL HISTOGRAM HOMOGENIZATION (Sheng H. L., 2015)**	**PROPOSED METHOD**
NIQE	4.170	6.674	3.800	4.085	3.582

(a) (b)

(c) (d)

(e) (f)

Figure 4.3: The effect of five haze removal methods: (a) Haze image, (b) DCP, (c) Fattal, (d) Retinex, (e) GHH, (f) Proposed method

NIQE quality evaluation score:

Table 4.3: Score of result of each method

	DCP (He K. M., 2011)	**FATTAL (Fattal R., 2008)**	**RETINEX (Fu X et al., 2014)**	**GLOBAL HISTOGRAM HOMOGENIZATION (Sheng H. L., 2015)**	**PROPOSED METHOD**
NIQE	3.769	4.981	3.580	3.667	3.518

4.5.2 Haze Image without Sky Region

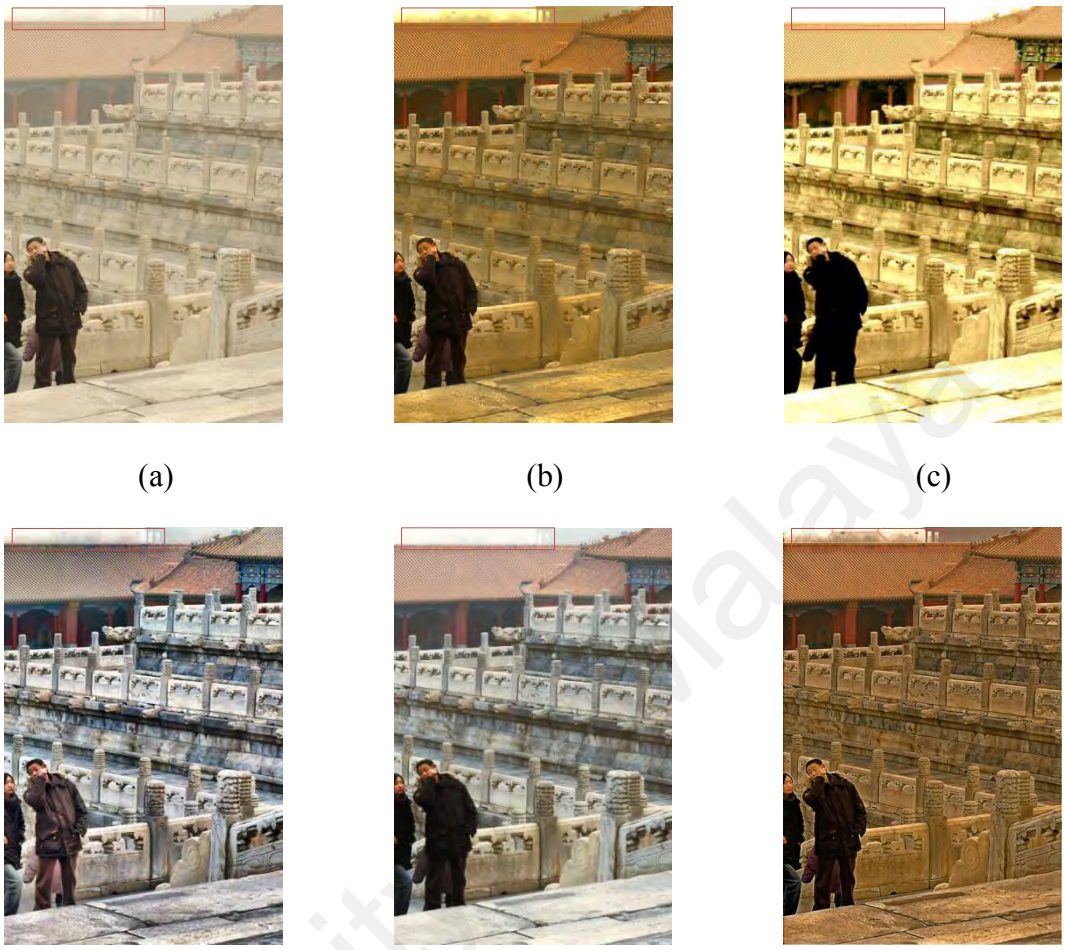

(a) (b) (c)

(d) (e) (f)

Figure 4.4: The effect of five haze removal methods: (a) Haze image, (b) DCP, (c) Fattal, (d) Retinex, (e) GHH, (f) Proposed method

As is clearly shown in the results, the proposed method has a better treatment effect on the distant scene in the red box above the image.

NIQE quality evaluation score:

Table 4.4: Score of result of each method

	DCP (He K. M., 2011)	**FATTAL (Fattal R., 2008)**	**RETINEX (Fu X et al., 2014)**	**GLOBAL HISTOGRAM HOMOGENIZATION (Sheng H. L., 2015)**	**PROPOSED METHOD**
NIQE	2.595	2.704	2.665	2.668	2.508

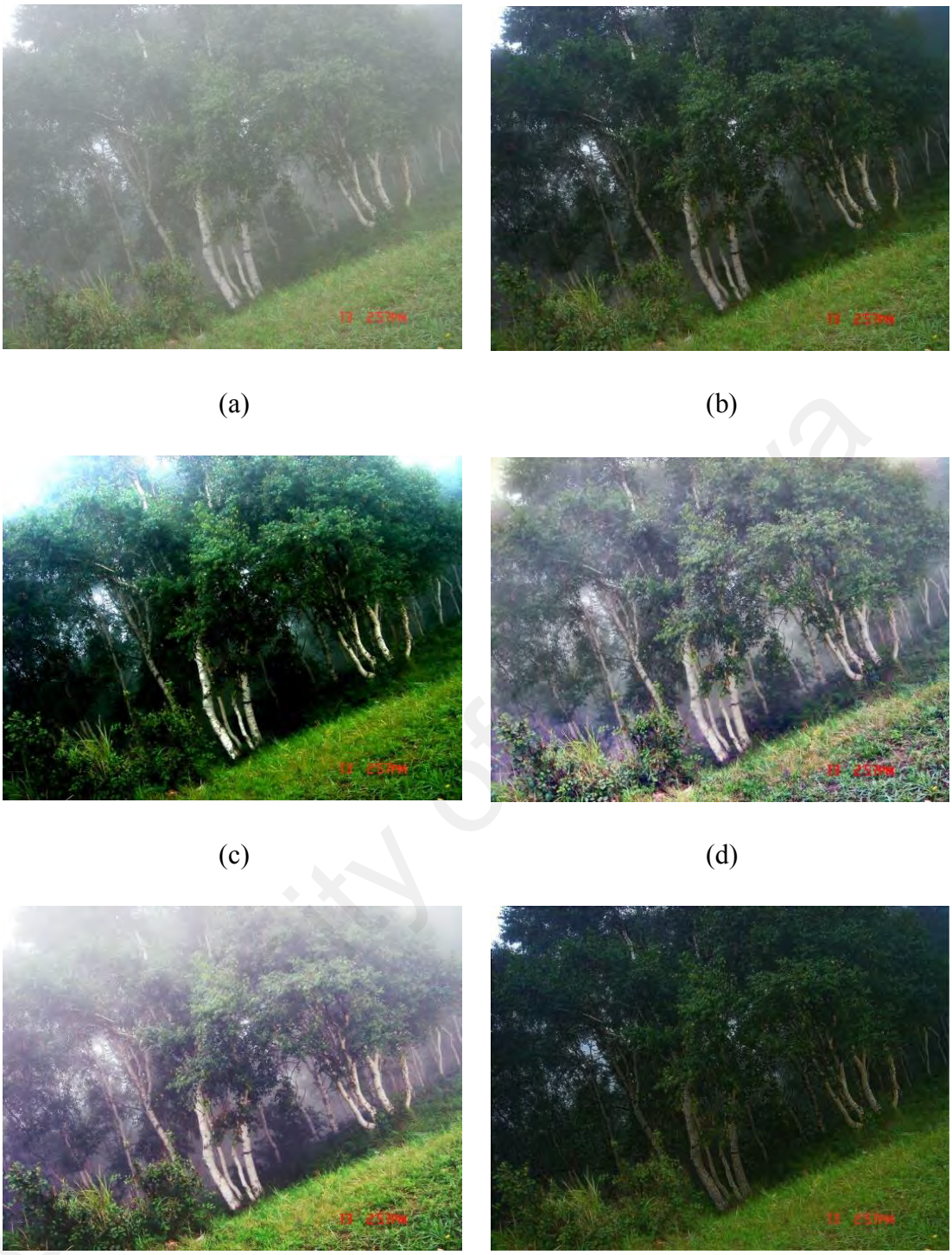

(a) (b)

(c) (d)

(e) (f)

Figure 4.5: The effect of five haze removal methods: (a) Haze image, (b) DCP, (c) Fattal, (d) Retinex, (e) GHH, (f) Proposed method

NIQE quality evaluation score:

Table 4.5: Score of result in each method

	DCP (He K. M., 2011)	**FATTAL (Fattal R., 2008)**	**RETINEX (Fu X et al., 2014)**	**GLOBAL HISTOGRAM HOMOGENIZATION (Sheng H. L., 2015)**	**PROPOSED METHOD**
NIQE	2.845	2.807	3.063	2.711	2.526

(a) (b)

(c) (d)

(e) (f)

Figure 4.6: The effect of five haze removal methods: (a) Haze image, (b) DCP, (c) Fattal, (d) Retinex, (e) GHH, (f) Proposed method

NIQE quality evaluation score:

Table 4.6: Score of result of each method

	DCP (He K. M., 2011)	**FATTAL (Fattal R., 2008)**	**RETINEX (Fu X et al., 2014)**	**GLOBAL HISTOGRAM HOMOGENIZATION (Sheng H. L., 2015)**	**PROPOSED METHOD**
NIQE	2.737	3.547	3.318	2.984	2.281

4.5.3 Haze Image Captured in the Highway

(a) (b)

(c) (d)

(e) (f)

Figure 4.7: The effect of five haze removal methods: (a) Haze image, (b) DCP, (c) Fattal, (d) Retinex, (e) GHH, (f) Proposed method

The result shows that this research can improve the recognition rate of vehicle and license plate under haze conditions.

NIQE quality evaluation score:

Table 4.7: Score of result of each method

	DCP (He K. M., 2011)	**FATTAL (Fattal R., 2008)**	**RETINEX (Fu X et al., 2014)**	**GLOBAL HISTOGRAM HOMOGENIZATION (Sheng H. L., 2015)**	**PROPOSED METHOD**
NIQE	5.834	4.325	4.634	4.957	3.986

4.6 Summary

Throughout this chapter, whether the proposed haze removal algorithm using improved restoration method based on dark channel prior is subjectively effective or objectively evaluated by using NIQE, the experimental results are better than those of other traditional haze removal algorithms.

The proposed algorithm in this research mainly improves the haze removal algorithm based on dark channel prior, which is intended to solve the limitations of edge blur and color distortion in the sky region.

CHAPTER 5

CONCLUSION

5.1 Research Discovery and Achievements

In the information society of the 21st century, people have made rapid progress in acquiring, processing and transmitting information. In the process of human information transmission, the image visual information occupies the majority. In many cases, images express and convey information more efficiently and quickly than other media. With the rapid progress of electronic technology and computer technology, the early image processing technology appeared in the middle of last century, and computers are becoming increasingly popular among people to process some image information. Digital image processing technology is widely used in the fields of aerospace, agricultural production, chemical engineering and computer vision, interwoven with other disciplines to promote development of each other. Nowadays, the research of image processing technology is more and more through, and the application of image processing technology is more and more extensive. However, due to the lack of understanding and cognition of human visual system, image processing technology itself still has many limitations, so the image processing technology needs further research and development.

This research mainly studies the haze removal technology of single image. At first, some classical haze removal algorithms are briefly introduced from the perspective of image enhancement technology and image restoration technology based on physical model. In the haze removal algorithm based on physical model, the reason of image

quality degradation and the physical model of image imaging in haze are analyzed. Then, the haze removal algorithm using physical model based on dark channel prior is introduced. Based on the analysis of the causes of the color distortion and edge blur in the sky and large bright region, this research proposed a haze removal algorithm using sky segmentation based on dark channel prior to settle the problem of color distortion in the sky and bright regions.

5.2 Conclusion

In this research, the haze removal algorithm based on dark channel prior is analyzed in depth, and the sky or large bright region in the haze image is segmented by the combination of gradient information and brightness information. This method can segment the sky region accurately.

By analyzed the phenomenon that the haze removal algorithm based on dark channel prior is wrong in estimating the transmittance of sky and large bright regions, this paper optimized the transmittance and atmospheric light value of the haze images containing sky and large bright regions. In order to solve the limitation of edge blur in the image processed by haze removal algorithm based on dark channel prior, different filters are adopted in method of dehaze-1 and method of dehze-2 in this research to replace the guided filter used in haze removal algorithm based on dark channel prior.

In general, the algorithm proposed in this research has a good effect of haze removal for haze images in different scenes. The results also show that this algorithm

has better haze removal effect than some other algorithms that proposed in this research.

To be specific, the results show that the proposed algorithm in this research solves the limitation of edge blur and color distortion in sky and large bright regions, also improved the robustness of the whole algorithm, as a results, all research objectives stated in Section 1.4 have been fulfilled.

5.3 Limitation and Future Work

Although the research in this research has achieved some results, but there are still some unsolved limitations in the research process. Such as:

i. The limitation of time-consuming

Aiming at the limitation of edge blur, this research used different filters in method of dehaze-1 and method of dehaze-2 to replace the guided filter used in haze removal algorithm based on dark channel prior, so more time is spent in filtering processing.

In addition, this research firstly segmented the sky region, and then respectively dehazing the haze images with sky region and without sky region. So this process also takes some time.

ii. The effect of haze removal in images with dense haze

According to the limitation of the atmospheric scattering physical model used in this research, the proposed algorithm used in this research has some limitations in the dense haze images.

Haze imaging is a complex system engineering, and its formation mechanism is affected by many factors. A single physical modeling cannot describe this process, and how to describe and express this physical process more accurately is the focus of the future work. On the other hand, improving the speed of overall haze removal algorithm is also the focus of attention in the future work.

REFERENCES

Blomgren P, Chan T F. (1998) Color TV: total variation methods for restoration of vector-valued images. IEEE Transactions on Image Processing A Publication of the IEEE Signal Processing Society, 7(3):304-309.

Brown E S, Chan T F. Bresson X. (2012), Completely Convex Formulation of the Chan-Vese Image Segmentation Model. International Journal of Computer Vision, 98(1):103-121.

Candes E, TAO T.(2006) Near- optimal signal recovery from random projections: Universal encoding strategies. IEEE transactions on information theory, 52(12): 5406- 5425.

Chen, K. (2017). Research of Defog Algorithm Based on Partial Differential Equation and Image Enhancement. *(Master's thesis, Xi'an University of Science and Technology, 2017).Electronic and Communication Engineering*.

Cheng F. C., Cheng C C, Lin P H, et al.(2015) A hierarchical airlight estimation method for imagefogremoval. Engineering Applications of Artificial Intelligence, 43: 27-34.

Chu H L, Li Y X, Zhou Z M, et al.(2013) Optimized Fast Dehazing Method Based on Dark Channel Prior. Acta Electronica Sinica, 41(4): 791-797.

Dai J, He K & Sun J. (2015) Convolutional Feature Masking for Joint Object and Stuff Segmentation. Proceeding of The Conference on Computer Vision and Paffter Regonition. Piscataway: IEEE.

Dong, Z. H. (2017). Image Haze Removal Improved Algorithm Using Dark Channel Prior. *(Master's thesis, Lanzhou Jiaotong University, 2017)*

Fan, F. B. (2016). Research on Algorithm of Haze Image Restoration. *(Master's thesis, Southwest University of Science and Technology, 2016)*

Fang Shuai, Zhang Jiqing, Cao Yang, et al. (2010) Improved Singe Image Dehazing Using Segmentation. Proceedings of IEEE International Conference on Image Processing.

Fattal, R. (2008). Single Image Dehazing. *ACM Transaction on Graphics, 27(3)*, pp. 721-729.

Fu X, Sun Y, Liwang M, et al. (2014) A Novel Retinex Based Approach for Image Enhancement with Illumination Adjustment. 1190-1194.

Gibson K B，Nguyen T Q. (2011) On the Effectiveness of the Dark Channel Prior for Single Image Dehazing by Approxi-mating with Minimum Volume Ellipsoids. Proceedings of IEEE International Conference on Acou-stics, Speech and Signal Processing. Washington D. C., USA: IEEE Press.

Gibson K B, Vo D T, Nguyen T Q.(2012) An Investigation of Dehazing Effects on Image and Video Coding. IEEE Transactions on Image Processing, 21(2):662-673.

Guo Fan, Cai Zixing, Xie Bin, et al.(2010) Review and Prospect of Image Dehazing Techniques. Journal of Computer Application. 20(9): 2417-2421.

Guo Xin.(2015) Color Image Segmentation Method of Statistical Region Merging. Journal of Xi'an University of Science and Technology, 35(3): 392-396.

Hauti'ere N, Tarel J P, Aubert D, et al.(2008) Blind Contrast Enhancement Assessment by Gradient Ratioing at Visible Edges. Image Analysis and Stereology Journal. 27(2): 87-95.

He, K. M., Sun, J., & Tang, X. O. (2009). Single Image Haze Removal Using Dark Channel Prior. *IEEE Conference on Computer Vision and Pattern Recognition*, pp. 1956-1963.

He, K. M., Sun, J., & Tang, X. O. (2011). Single Image Haze Removal Using Dark Channel Prior. *IEEE Transactions on Pattern Analysis and Machine*

Intelligence, pp. 2341-2353.

Hitam M S, Yussof W N J H W, Awalludin E A, et al., Mixture Contrast Limited Adaptive Histogram Equation for Underwater Image Enhancment, in *International Conference on Computer Applications Technology*. IEEE, 2013, pp. 1-5.

Huang K Q, Wang Q & Wu Z Y. (2006) Natural Color Image Enhancement and Evaluation Algorithm Based on Human Visual System. Computer Vision and Image Uderstanding. 103(1):52-63.

Inampud R B, Purimetla T N & Satyanarayana P G.(2002) Contrast degradation for improving quality of an image. Geoscience and Remote Sensing Symposium, 6:3408-3410.

Jiang, Y. T., Sun, C. M., Zhao, Y., & Yang, L. (2017). Image Dehazing Using Adaptive Bi-channel Prior on Superpixels. *Computer Vision and Image Understanding, ScienceDirect*, pp. 17-32.

Jin Hwan Kim, Won Dong Jang, Jae Young Sim & Chang Su Kim.(2013) Optimized contrast enhancement for real-time image and video dehazing. Journal of Visual Communication and Image Representation. 2013 (3)

Kim J H, Jiang W D, Sim J Y, et al. (2013) Optimized Contrast Enhancement for Real-time Image and Video Dehazing. *Journal of Visual Communication & Image Representation*. Vol. 24, no. 3, pp. 410-425.

Kim J Y, Kim L S, Hwang S H. (2001) An Advanced Contrast Enhancement Using Partially Overlapped Sub-block Histogram Equation, *IEEE Transactions on Circuits & System for Video Technology*, vol. 11, no. 4, pp. 475-484.

Land E H, McCann J J. (1971) Lightness and Retinex Theory. Josa, 61(1):1-11.

Land E H. (1977) The Retinex Theory of Color Vison. Scientific America.

Leng, J. W., & Li, P. (2017). Single Image Defogging Algorithm Based High-Order Markov Random Fields. *Journal of Graphics, 38*, pp. 745-753.

Levin A, Lischinski D & Weiss Y. (2006) A Closed Form Solution to Natural Image Matting. Proceedings of IEEE Computer Society Conference on Computer Vision and Pattern Recognition. Washington D. C., USA:IEEE Press.

Lin, X. G. (2017). A Fast Image Haze Removal Based on Dark Channel Prior. *(Master's thesis, Zhengzhou University, 2017).Institute of Physical Science and Engineering*.

Liu, C. (2016). The Application of Curvelet Transform in Image Dehazing Processing. *(Master's thesis, Yunnan University, 2016)*

Liu T，Zhang W & Yan S Z. (2015) A novel image enhancement algorithm based on stationary wavelet transform for infrared thermography to the de-bonding defect in solid rocket motors. Mechanical Systems and Signal Processing, 62: 366-380.

Long J, Shelhamer E & Darrell T. (2015) Fully Convolutional Networks for Semantic Segmentation. IEEE. Proceedings of The Conference on Computer Vision and Pattern Recognition Piscataway: IEEE.

Long W, Liang X, Cai S, et al. (2016) A modified augmented Lagrangian with improved grey wolf optimization to constrained optimization problems. Neural Computing & Applications, 2016:1-18.

Mao Tianyi, Optimizing Technology of Dark Channel Prior Dehazing Based on Sky Region Segmentation. Nanjing University of Aeronautics and Astronautics.

McCartney E J.(1975) Optics of Atmosphere: Scattering by Molecules and Particles. John Wiley and Son.

McCartney E J. (1977) Optics of the atmosphere: scattering by molecules and particles. Journal of Modern Optics, 14 (7): 521-521.

Mittal, A., R. Soundararajan, and A. C. Bovik. "Making a Completely Blind Image Quality Analyzer." IEEE Signal Processing Letters. Vol. 22, Number 3, March 2013, pp. 209–212.

Narasimhan S G, Nayar S K. (2002) Vision and the Atmosphere. International Journal of Computer Vision, 48(3):233-254.

Narasimhan S G, Nayar S K. (2000) Chromatic Framework for Vision in Bad Weather. Proceeding of IEEE Conference on Computer Vision and Pattern Recognition (CVPR). Hilton Head Island, SC, USA: IEEE Computer Society.

NarasimhanGS, & NayarKS. (2003). Interactive De-weathering of an Image Using Physical Model. IEEE Workshop on color and Photometric Methods in Computer Vision.

Oakley, J. P., & Satherley, B. L. (1988). Improving Image Quality in Poor Visibility Conditions Using Model for Degradation. *IEEE Transaction on Image Processing*, pp. 167-179.

Otsu N. (1975) A Threshold Selection Method From Gray-level Histograms. Automatica. 11(285-296): 23-27.

Pei Soo-Chang, Lee Tzu-Yen,(2012) Effective Image Haze Removal Using Dark Channel Prior and Post-Processing. *Proceedings of IEEE International Symposium on Circuits and System. Washington D. C., USA:IEEE Press* 2777-2780

Peli, E. (1990) Contrast in complex images. J. Opt. Soc. Am. A 7 (10), 2032–2040.

Russo F., (2002) An Image Enhancement Technique Combining Sharping and Noise Reduction. *IEEE Transactions on Instrumentation and Measurement*, vol. 51, no. 4, pp. 824-828.

Sahoo S K，Makur A. (2015) Enhancing image denoising by controlling noise incursion in learned dictionaries. IEEE Signal Processing Letters，22（8）：1123-1126.

S C Huang, B H Chen, W J Wang. (2014) Visibility Restoration of Single Hazy Images Captured in Real-World Weather Conditions. IEEE Transactions on Circuits and Systems for Video Technology, 24(10):1814-1824.

Seow M J, Asari V K. (2006). Ratio Rule and Homomorphic Filter for Enhancement of Digital Colour Image [J]. Neuro Computing, 69(7):954-958.

Sheng H. L., Isa N. A. M., Chen H. O., et al. (2015) A New Histogram Equalization Method for Digital Image Enhancement and Brightness Preservation. Signal, Image and Video Processing, 9(3): 675-689.

Shi, L., Yang, L., Chu, S. B., Yang, J. X., Yang, Y., Zhao, B., & Fu, M. Y. (2017). Image Haze Removal Using Dark Channel Prior and Minimizing Energy Function. *IEEE*.

Soo-Chang Pei, Tzu-Yen Lee. Effective image haze removal using dark channel prior and post-processing. In Circuits and Systems (ISCAS), 2012 IEEE International Symposium on, pages 2777–2780. IEEE, 2012.

Stone T, Mangan M, Ardin P, et al. (2014) Sky Segmentation with Ultraviolet Images Can be Used for Navigation. Proceedings Robotics: Science and System.

Sun, W., Wang, H., Sun, C., Guo, B., Jia, W., Sun, M., 2015. Fast single image haze removal via local atmospheric light veil estimation. Comput. Electr. Eng. 46, 371–383.

Tang L, Chen S, Liu W, et al. (2011) Improved Retinex Image Enhancement Algorithm. *Procedia Environmental Sciences*, vol. 11, Part A, pp. 208-212.

Tan, R. (2008). Visibility in Bad Weather From a Single Image. *Proceedings of IEEE Conference on Computer Vision and Pattern Recognition*, pp. 2347-2354.

Tan K K, Oakley J P. (2001) Physical-based Approach to Color Image Enhancement in Poor Visibility Conditions. JOSAA, 18(10):2460-2467.

Tarel J P & Hautiere N. (2009) Fast Visibility Restoration From a Single Color or Gray Level Image. Computer Vision, 2009 IEEE 12th International Conference omn. IEEE.

Tarel, J.P., Hautiere, N., Cord, A., Gruyer, D., Halmaoui, H., 2010. Improved visibility of road scene images under heterogeneous fog. IEEE Intelligent Vehicles Symposium (IV'10). pp. 478–485.

Tarel. (2015, September 15) Single Image Visibility Restoration Comparision. Retrieved November 17, 2018, from http://perso.lcpc.fr/tarel.jean-philippe/visibility/.

Ti Xuan, Li Zhao xu, Guo Xin yun. (2018). A Sky-distinguish Improved Dehazing Algorithm Based on Dark Channel Prior. *Information Technology and Informatization*. 100-103.

Ullah E, Nawaz R & Iqbal J. (2013) Single Image Haze Removal Using Improved Dark Channel Prior. Medeling. Identification & Control (ICMIC). Proceedings of International Conference on. IEEE.

Wang, K., Dunn, E., Tighe, J., Frahm, J.-M., 2014. Combining semantic scene priors and haze removal for single image depth estimation. IEEE Winter Conference on Applications of Computer Vision (WACV). pp. 800–807.

Wang, W. C., Chang, F. L., Ji, T., & Wu, X. J. (2018). A Fast Single-Image Dehazing Method Based on a Physical Model and Gray Projection. *Special Section on Cyber-Physical-Social Computing and Networking,IEEE*, pp. 5641-5653.

Wang, Y. C. (2011). Research on Haze Removal Using Dark Channel Prior. *(Master's thesis, Dalian University of Technology, 2011)*

Wang Z, Bovik A C, Sheikh H R, et al. (2004) Image Quality Assessment From Error

Visibility to Structural Similarity. IEEE Transactions on Image Processing. 13(4):600-612.

Wu di & Zhu Qingsong. (2011) The Latest Research Progress of Image Dehazing. Journal of Image and Graphics. 16(9): 1561-1576.

Wu Yanhai, Pan Chen, Wu Nan. Single Image Dehazing Based on an Improved Recursive Segmentation of Otsu Algorithm. Journal of Xi'an University of Science and Technology, 2017, 37(3):438-444.

Wu yan hai, Pan chen, Wu nan. (2017). Research on Improved Otsu Recursively Segmented Single Image Dehazing Algorithm. *Journal of XI'An University of Science and Technology*. 438-444

Zhang G, Yan P, Zhao H, et al. (2008) A Survey of Image Enhancement Algorithms Based on Retinex Theory. in *The Third International Conference on Computer Science & Education*.

Xiao Chunxia & Gan Jiajia. (2012) Fast Image Dehazing Using Guided Joint Bilateral Filter. Journal of Visual Computer, 28(6-8):713-721.

Xiao F, Wang H M & Zhang Y G. (2014) Multi-scale local region based level set method for image segmentation in the presence of intensity inhomogeneity. Neurocomputing.

Xiao Shengbi & Li Yan. (2015) Haze Removal Algorithm based on Fast Multi-scale Retinex with Color Fidelity. Computer Engineering and Application. 51(06):176-180.

Zhu Q, Mai J & Shao L. (2015) A Fast Single Image Haze Removal Algorithm Using Color Attenuation Prior. *IEEE Transactions on Image Processing*. 24(11):3522-3533.

Zuo Z, Lan X, Zhou G, et al. (2012) A Time Dependent Modelvia Non-Local Operator for Image Restoration. the seventh international conference on intelligent

system and knowledge engineering, iske/ the 1st international conference on cognitive system and information processing, csip.